Developmental Biology 344 (2010) 1071–1087

Contents lists available at ScienceDirect

Developmental Biology

journal homepage: www.elsevier.com/developmentalbiology

Genomes & Developmental Control

# Comparative gene expression analysis of genital tubercle development reveals a putative appendicular Wnt7 network for the epidermal differentiation

Han Sheng Chiu [a], John C. Szucsik [b], Kylie M. Georgas [a], Julia L. Jones [c], Bree A. Rumballe [a], Dave Tang [a], Sean M. Grimmond [a], Alfor G. Lewis [b], Bruce J. Aronow [b,c], James L. Lessard [b], Melissa H. Little [a,*]

[a] Institute for Molecular Bioscience, The University of Queensland, St. Lucia 4072, Australia
[b] Division of Developmental Biology, Cincinnati Children's Hospital Research Foundation, Cincinnati, OH 45229, USA
[c] Division of Biomedical Informatics, Cincinnati Children's Hospital Research Foundation, Cincinnati, OH 45229, USA

ARTICLE INFO

*Article history:*
Received for publication 30 November 2009
Revised 23 April 2010
Accepted 15 May 2010
Available online 24 May 2010

*Keywords:*
Genital tubercle development
Lower urinary tract development
Gene expression
Wnt
Appendage development

ABSTRACT

Here we describe the first detailed catalog of gene expression in the developing lower urinary tract (LUT), including epithelial and mesenchymal portions of the developing bladder, urogenital sinus, urethra, and genital tubercle (GT) at E13 and E14. Top compartment-specific genes implicated by the microarray data were validated using whole-mount *in situ* hybridization (ISH) over the entire LUT. To demonstrate the potential of this resource to implicate developmentally critical features, we focused on gene expression patterns and pathways in the sexually indeterminate, androgen-independent GT. GT expression patterns reinforced the proposed similarities between development of GT, limb, and craniofacial prominences. Comparison of spatial expression patterns predicted a network of *Wnt7a*-associated GT-enriched epithelial genes, including *Gjb2*, *Dsc3*, *Krt5*, and *Sostdc1*. Known from other contexts, these genes are associated with normal epidermal differentiation, with disruptions in *Dsc3* and *Gjb2* showing palmo-plantar keratoderma in the limb. We propose that this gene network contributes to normal foreskin, scrotum, and labial development. As several of these genes are known to be regulated by, or contain cis elements responsive to retinoic acid, estrogen, or androgen, this implicates this pathway in the later androgen-dependent development of the GT.



## Introduction

Congenital anomalies of the urogenital tract are the third most common birth defects, with abnormalities of the external genitalia being the most prevalent manifestation. Cryptorchidism (undescended testes) and hypospadias (in which the urethral orifice is located on the underside of the penis or at the perineum) each occur in as many as 1 in 125 males born (Kurzrock et al., 1999; Cox et al., 2008) and the prevalence of these two conditions appears to be rising, potentially due to environmental exposure to anti-androgenic compounds (Miyagawa et al., 2002; Brouwers et al., 2007; Wang and Baskin, 2008). These and other less common anomalies of the external genitalia (diphallia, micropenis) create social as well as reproductive challenges for the affected individuals. The lower urinary tract (LUT) is defined as extending from the bladder to the meatal opening of the urethra. Congenital anomalies of the kidney and urinary tract (CAKUT) include such defects as vesicoureteric reflux (VUR; improper insertion of the ureters into the bladder) and posterior urethral valves (fine outgrowths of urethral tissue that result in bladder outlet obstruction; Kerecuk et al., 2008). Such conditions are quite common (VUR presents in 1–2% of all children; Kerecuk et al., 2008), with the sequelae of most LUT problems presenting later in life (urge incontinence, stress incontinence, cystitis, neurogenic bladder, overactive bladder, erectile dysfunction) and being etiologically poorly understood.

Despite a physiological relationship with the mesodermally derived kidney and ureters, the LUT and GT have distinct embryological origins. The LUT develops from the endodermal cloaca, which becomes separated into the urogenital sinus and rectum by the downgrowth of the urorectal septum around E10.5 in mouse. The urogenital sinus gives rise to the internal urethra and bladder. While both become lined with a water-tight urothelial layer, these two regions differentiate into distinct structures with respect to musculature, stroma, epithelial layers, and innervation. The role of the LUT is storage and voiding. Regulation of appropriate micturition requires complex neural connections and, unlike most internal organs, control of storage and voiding by the LUT involves voluntary regulation. Locally, this involves sympathetic and parasympathetic innervation of the bladder and somatic motor nerves to regulate contraction of the urethral sphincter (Fowler et al., 2008). As well as providing a barrier, the urothelial cells of the bladder also act as mechanosensors and are actively involved in triggering neural

* Corresponding author. Fax: +61 7 3346 2101.
*E-mail address:* M.Little@uq.edu.au (M.H. Little).

0012-1606/$ – see front matter © 2010 Elsevier Inc. All rights reserved.
doi:10.1016/j.ydbio.2010.05.495

responses in response to bladder expansion. The importance of the urothelium in this process was recently highlighted by the presence of urothelial hyperplasia and non-voiding contractions in bladders from mice defective for either uroplakin II or IIIa (Aboushwareb et al., 2009). The genital tubercle (GT) gives rise to the male and female external genitalia (penis, clitoris, scrotum, labia, foreskin) and represents the intersection between the reproductive and urinary tracts. The primary swellings of the genital tubercle form the penis and clitoris, while the preputial swellings give rise to the foreskin in males and the labia minora in females. A second set of swellings, the labioscrotal swellings, arise later in development and give rise to the scrotum and labia majora in males and females, respectively. The LUT and GT physically intersect as the urethra passes through the GT. The GT is proposed to be derived from all three germ layers. The urethral plate (UP) is derived from urethral endoderm (Siefert et al., 2008). The GT surface other than the urethral plate is derived from surface ectoderm and the core of the extending appendage is derived from lateral plate mesoderm (Perriton et al., 2002). Murine GT development commences at approximately E10.75, with the appearance of paired swellings ventral to the cloacal membrane (Perriton et al., 2002). Without a urethral plate, the GT will fail to form. The urethral epithelium of the GT does not grow out from the urethra but forms *in situ* along the GT itself (Pennington and Hutson, 2002). GT development involves an early androgen-independent phase and a later androgen-dependent phase, after which sexual dimorphism is evident. In mouse, this dimorphism is not evident until approximately E16, before which there has already been significant outgrowth and patterning during an androgen-independent phase.

The genital tubercle develops as an out-budding appendage, hence it has been proposed that there is congruence in the genetic basis of GT patterning with other out-budding appendages, including the limb and craniofacial prominences. Of these three appendages, limb patterning has been most highly studied. The limb has three key axes of development, the anterior–posterior axis (thumb to little finger), proximal–distal axis (arm to finger tips), and dorsal–ventral or plantar–palmar (back of hand to palm) axis. Major growth factor pathways involved in limb development include the hedgehog, fibroblast growth factor (FGF), bone morphogenetic protein (BMP) pathways, and Wnt pathways (Goodman et al., 2000; Ahn et al., 2001; Hill et al., 2006; Geetha-Loganathan et al., 2008; Witte et al., 2009). Sonic hedgehog (*Shh*) is expressed in a posterior zone of polarizing activity (ZPA) and is critical for limb anterior–posterior (A–P) patterning. Duplication of this region on the anterior side of the limb leads to a mirror image duplication of digits (polydactyly). Extension in the distal direction involves signals from the apical ectodermal ridge (AER), notably *Fgf8*, but also *Fgf4*, *Fgf9*, and *Fgf17* (Mariani et al., 2008). These same signaling pathways are involved in GT development. Here, *Shh* is expressed in the endodermal UP along the ventral surface of the GT (Haraguchi et al., 2001; Perriton et al., 2002). The UP has been proposed to act as an organizing center similar to the ZPA in the limb. Transplantation of this region into the anterior limb of the chick induces digit duplication; however, it also results in the dimpling of the skin and formation of a furrow similar in structure to the UP (Haraguchi et al., 2001; Perriton et al., 2002). The UP expression of *Shh* influences the development of the adjacent mesenchyme, eliciting extension to form the GT. Shh was proposed to regulate the expression of *Fgf8* and *Bmp7*, which are also expressed in the UP and distal urethral epithelium (DUE), and *Wnt5a*, *Bmp2*, *Bmp4*, and *Fgf10*, which are expressed in the mesenchyme surrounding the urethral plate (Yamaguchi et al., 1999; Haraguchi et al., 2000; Perriton et al., 2002). Expression of *Shh* is required throughout the period of androgen-independent GT extension. By removing *smoothened* from different layers of the developing GT, it was also demonstrated that the primary target of Shh is the GT mesenchyme (Lin et al., 2009). *Shh* knockout mice show a loss of GT accompanied by a loss of expression of *Bmp4* and *Fgf10*, suggesting that Shh is upstream of both of these growth factor pathways. As for the limb, the GT undergoes considerable proliferative extension prior to structural differentiation. In the limb, this outgrowth is driven by the expression of *Fgf8* in the AER. The expression of *Fgf8* in the DUE was similarly presumed to be required for GT extension and outgrowth (Morgan et al., 2003; Yamada et al., 2006). Certainly the presumptive region of *Fgf8* expression is lost when *Shh* is deleted. Surprisingly, the conditional removal of *Fgf8* from the cloacal and urethral epithelium did not affect GT outgrowth, even though there was a loss of expression of putative downstream targets of *Fgf8* (*Bmp4*, *Wnt5a*, *Hoxd13*) and no evidence of a redundant role for other members of the Fgf family (Siefert et al., 2009). Wnt5a has been shown to be involved in outgrowth of GT and limb (Yamaguchi et al., 1999). The loss of *Shh* also reduces canonical Wnt signaling demonstrating that anterio-posterior extension due to mesenchymal proliferation likely require Wnt signaling from the DUE (Miyagawa et al., 2009). Indeed, concommitent loss of *Shh*, *Wnt5a*, and *axin2* expression is seen in two models of disrupted GT and anorectal development, Danforth's short tail (Sd) and all-trans RA-treated mice (Nakata et al., 2009).

GT expression of Shh also regulates Hoxd13 and Hoxa13 expression, although independently to Wnt and Fgf signaling. (Lin et al., 2009). The homeodomain genes *Hoxa13* and *Hoxd13* are also expressed in the UP, whereas *Msx1* and the Shh receptor, *Ptch1*, are expressed in the surrounding mesenchyme. Here again, there is a similarity to limb where *Hoxa13* and *Hoxd13* are required for the development and A–P patterning of the autopods (digits; Cobb and Duboule, 2005). Homozygote knockouts of these genes result in loss of the limbs and phallus, whereas heterozygotes display disrupted patterning in both locations (reviewed in Perriton et al., 2002). In humans, mutations in these genes result in hand–foot–genital syndrome (Goodman et al., 2000). In the posterior embryo, these homeodomain genes also control formation of the terminal vertebrae and the anus. The UP is therefore also thought to be critical for both dorsal–ventral patterning and proximal–distal extension of the GT.

As noted, congenital GT defects are very common. Based on observations in mice, hypospadias may result from disruptions in *Fgfr2*, *Fgf8*, *Fgf10*, and B*mp7*, all of which are involved in UP patterning (Beleza-Meireles et al., 2007). In humans, hypospadias has been observed in Opitz syndrome (*MID1* mutation), Pallister–Hall syndrome (*GLI3* mutation), Reiger syndrome, type 1 (*PITX2* mutation), Hand–foot–genital syndrome (*HOXA13*, *HOXD13* mutations), and split-hand/split-foot malformation type 1 and type 4 (mutations in Dlx5, Dlx6, and Dss1; Yamada et al., 2006; Suzuki et al., 2008). Micropenis occurs in Pallister–Hall syndrome, Robinow syndrome (*ROR2* mutation), Ulnar mammary syndrome (*TBX3* mutation), and X-linked lissencephaly (*ARX* mutation; reviewed in Yamada et al., 2006). Mutations in CXorf6 have also been identified in isolated cases of non-syndromic hypospadias (Kalfa et al., 2008).

Despite the clinical relevance and prevalence of defects, there have been almost no systems biology applied to the molecular basis of LUT/GT development. Li et al. (2006) performed expression analysis of mouse GT (E14, E15, E16, and E17) but focused on those genes expressed during the later androgen-dependent phase of development. In this study, we have addressed this gap by creating a comprehensive data set of microarray and *in situ* gene expression of the E13 and E14 LUT/GT. In order to test the utility of this data set, we analyzed in more depth gene expression in the GT. Ontological analysis of GT-enriched genes reaffirmed the importance of Wnt signaling and defined an epidermal, estrogen-responsive, *Wnt7a*-associated gene network potentially involved in foreskin/labial development and possibly defective in hypospadias (Table 1).

**Table 1**
Overview of ToppGene ontological analysis of the most active genes in each compartment of the developing LUT examined. For each category, features that are common between different compartments are highlighted in distinct colors to assist in visual assessment of similarities between compartments. No pathways were strongly evident in E13 urethral mesenchyme, E13 bladder mesenchyme, or E14 bladder. No human phenotypes were linked to genes expressed in the E13 bladder mesenchyme.

| | E13 Ureth Epith | E13 Ureth Mesen | E13 Bladder Epith | E13 Bladder Mesen | E14 GT | E14 Urethra | E14 UGS | E14 Bladder |
|---|---|---|---|---|---|---|---|---|
| Molecular Function | TF activity | TF activity | TF activity | VEGFR binding | TF activity | TF activity | calcium ion binding | TF activity |
| | structural molecules | calcium ion binding | cytoskeleton | DNA binding | calcium ion binding | calcium ion binding | TF activity | TGF beta binding |
| | calcium ion binding | ephrin R activity | Cl channel activity | calmodulin binding | chromatin binding | chemorepellant | receptor protein kinase | transferase activity |
| Biological Process | epithelial / epidermal devel | neural development | epithelial / epidermal dev | axon guidance | limb / appendage devel | neural development | neural development | lung development |
| | cell adhesion | cell adhesion | regulation of transcription | cell motion / localisation | neural development | cell-cell adhesion | cell adhesion | epithelial development |
| | regulation of transcription | axonogenesis | autonomic NS / neural crest | cell adhesion | cell adhesion | tube development | axonogenesis | reguation of transcription |
| Cellular Component | apicolateral junction | neuron projection | apicolateral junction | extracellular matrix | plasma membrane | extracellular space | neuron projection | extracellular matrix |
| | cell junction | synapse | cell-cell junction | chromosome passenger complex | cell-cell junction | plasma membrane | intrinsic to plasma memb | extracellular space |
| | intercalated disc | plasma membrane | basolaternal membrane | extracellular space | intercalated disc | extracellular matrix | nucleosome | plasma membrane |
| Domain | cadherin | cadherin | plectin | bZIP | cadherin | cadherin | cadherin | ETS domain 3 |
| | bZIP | nuclear orpan receptor | marvel | TSP1 | homeobox | forkhead | stathmin | ZnF GATA |
| | Plectin | stathmin | LDLa | HELP | OAR | thyroglobulin | FnIII | FnIII |
| Pathway | cadherin signaling | | breast cancer E2signaling | | wnt signaling | cadherin signaling | cadherin signaling | |
| | wnt signaling | | cell adhesion | | cadherin signaling | wnt signaling | wnt signaling | |
| | breast cancer E2 signaling | | tight junction | | basal cell carcinoma | axon guidance | SLE | |
| Human Phenotype | abnormal keratinisation | Hirschsprung disease | abnormality of the uterus | onset in 1st or 2nd decade | abnormal phalanges / limb | abnormality of face | renal dysplasia / VUR | cardiovascular dilatation |
| | abnormalities of skin | Anal stenosis | renal dysplasia | | hyperkeratosis | external genital abnorm | genital abnormality | muscular hypotonia |
| | abnormal mouth / teeth | Abnormal limb musc | cutaneous syndactyly | | abnormality of the head / face | abnormality of phalanges | polydactyly | molluscoid pseudotumors |
| Mouse Phenotype | abnormal skin morphology | abnormal neurons | abnormal mesonephros morpholc | impaired smooth muscle | abnormal limb | perinatal lethality | abnormal neuron | absent tracheal rings |
| | abnormal vagus ganglion | abnormal musculature | abnormal epidermis morph | abnormal umbilical artery | abnormal face / mouth / head | abnormal oral / facial | neonatal lethality | abnormal ischium |
| | abnormal esophagus morph | perinatal lethality | thickened epidermis | abnormal skeleton | abnormal skeleton | abnormal digestive sys | conductive hearing loss | abnormal vertebrae |
| Disease | Epidermolysis Bullosa | Hirschsprung Disease | renal adysplasia | autistic disorder | autistic disorder | salivary gland neoplasms | salivary gland neoplasms | Autistic Disorder |
| | Keratoderma, Palmoplantar | Autistic Disorder | nonsyndromic cleft lip +/-palate | hypertrophic neuropathy | Branchio-Oto-Renal syn | Branchio-Oto-Renal syn | Branchio-Oto-Renal syn | Ehlers-Danlos Type 2 |
| | neoplasia | Waardenburg Shah syn | prostate cancer | oral submucous fibrosis | Epidermolysis Bullosa | autonomic control loss | Williams Syndrome | oral submucous fibrosis |
| | insulin resistance | protein QT loci | infertility, male | intervertebral disc disease | female UG disease | head / neck Neoplasms | Autistic Disorder | reperfusion Injury |
| | infertility, male | Pheochromocytoma | prostatic neoplasms | pulmonary function traits | Keratoderma, Palmoplantar | neoplasm metastasis | Hirschprung disease | Obesity |

VEGFR: vascular endothelial growth factor receptor; SLE: systematic lupus erythematosis; VUR: vesicoureteric reflux; QT: quantitative trait; TGF: transforming growth factor; CI: chloride.

## Materials and methods

### *Collection of material for expression profiling*

At E13.5, a pregnant female FVB/N mouse was sacrificed by $CO_2$ asphyxiation, and following a midline abdominal incision, the gravid uteri were removed and placed in PBS on ice. Embryos were dissected under magnification. Bladder and urethra were dissected free of surrounding tissues and then divided at the level of ureteral insertion. Bladder segments were incubated in 20 mM EDTA in Tyrode's solution for 20 min at 37 °C. Urethral segments were treated with Trypsin (1 mg/ml in PBS) for 20 min (37 °C). In each instance, epithelium was separated from mesenchyme by rimming with a fine needle. Tissues were then placed in RLT Buffer containing ß-ME, according to manufacturer's instructions (RNeasy Micro Kit, Qiagen, Valencia, CA) and rapidly frozen in dry ice prior to storage at −80 °C for subsequent RNA purification. This was achieved using a spin-column system (RNeasy Micro Kit, Qiagen, Valencia, CA), according to manufacturer's directions, and stored at −80 °C prior to amplification.

At E14, a pregnant female FVB/N mouse carrying the SMGA/EGFP transgene (Szucsik et al., 2004) was sacrificed by $CO_2$ asphyxiation, and following a midline abdominal incision, the gravid uteri were removed and placed in PBS on ice. Embryos were dissected under GFP illumination. The lower urinary tract was trisected into bladder (EGFP positive dome), UGS (EGFP negative), and urethra (EGFP positive). A separate, non-transgenic pregnant FVB/N female was used to obtain samples of the genital tubercle at E14. Tissues were rapidly frozen in dry ice and stored at −80 °C for subsequent RNA purification using a spin-column system (RNeasy Micro Kit, Qiagen, Valencia, CA), according to manufacturer's directions, and stored at −80 °C prior to amplification.

### *Expression profiling, data normalization, and analysis*

Purified RNA was analyzed for concentration and integrity using the Agilent RNA 6000 Pico Kit (Agilent Technologies, Santa Clara, CA) and then 0.5–1.5 ng (in a volume of 1 µl) underwent two-round amplification (Epicenter Biotechnologies, Madison, WI) according to manufacturer's directions except for the addition of Full Spectrum™ multistart primers (SBI System Biosciences, Mountain View, CA) per the manufacturer's directions. The resultant product was biotinylated and hybridized to Affymetrix Mouse MOE 430 2.0 microarray chips (Affymetrix, Santa Clara, CA). CEL files were generated using Expression Console v1.1.1 (Affymetrix) and subjected to RMA normalization using Affymetrix CDF probe set definitions and GeneSpringGX v7.3.1 (Agilent). The relative expression of each probe set in each sample was calculated as the ratio relative to the median of its values as measured across the entire GUDMAP MOE 430 2.0 data set that contains developing and postnatal tissues from kidney, lower urinary tract, and gonadal tissues. Probe sets to be analyzed for differential expression across the developing lower urinary tract samples were then selected by filtering for those with RMA expression intensity greater than 6.2 in at least two replicates from any sample type. A general ANOVA was used to identify probe sets that are differentially expressed between sample types with less than 5% false discovery using Benjamini Hochberg *p*-value correction. From the resulting 18K probe sets, those with highest relative expression in the genital tubercle were identified based on normalized expression as referenced to the diverse panel of other developing and postnatal genitourinary samples. GeneSet enrichment analysis was performed using ToppGene (Chen et al., 2009). Genes that exhibited shared properties with respect to gene set enrichment features were transformed into network representations using CytoScape as previously described (Brunskill et al., 2008) using the ToppCluster server (http://toppcluster.cchmc.org/; Kaimal et al., submitted).

### *Collection of material for in situ hybridization*

For *in situ* hybridization, outbred CD1 embryos were collected from two time points, TS17 (10.5 dpc) and TS21 (13.5 dpc), where 0.5 dpc was defined as noon of the day on which mating plug was observed. Embryos were dissected in ice-cold PBS under a dissecting microscope and fixed in fresh 4% paraformaldehyde (PFA) at 4 °C overnight. Tissues were then washed in PBTX and dehydrated through a PBTX/methanol series (25%, 50%, 75%) and stored in 100% methanol at −20 °C until usage. TS17 whole embryos were collected with a puncture in the back of the head to prevent subsequent stain trapping in the brain. Tail somites were counted for TS17 litters to confirm embryos are within the range of 35–39 somites, as described by Kaufman et al. (1994). The lower urogenital system plus genital tubercle were collected from TS21 and sex was determined by gonadal inspection.

### *Riboprobe synthesis*

The complete protocol for digoxigenin (Dig)-labeled riboprobe synthesis is available and described in detail on the GUDMAP gene expression database (http://www.gudmap.org/Research/Protocols/Little.html). A brief overview, with minor changes to the protocol, is described here. Primers were ordered from Invitrogen according to the microarray output and were designed to amplify a 3′ UTR region of a gene between 500 and 800 bp. Riboprobes were amplified from either the Fantom II plasmid pool or the combination of both 12.5- and 15.5-dpc whole embryonic mouse cDNA. The 3′ primers were tagged with a T7 polymerase sequence, which allows *in vitro* transcription of Dig-labeled riboprobes using T7 RNA polymerase (Roche). Riboprobes were then purified with lithium chloride precipitation. A master mix was made with each riboprobe consisting of: 4 M LiCl (10 µl), 0.2 M EDTA, pH 7 (8 µl), 100% ethanol (300 µl), and water (100 µl) and stored at −20 °C overnight. Samples were then spun for 20 min at 13,000 rpm at 4 °C with supernatant discarded after the spin. Samples were gently washed with 1 ml of chilled 70% ethanol, then spun for 5 min at 13,000rpm at 4 °C. Supernatants were discarded and samples dried for 10 min at room temperature. Pellets from each sample were resuspended with 25 µl of water and stored at −70 °C.

### *Whole-mount in situ hybridization and imaging of WISH*

The complete protocol for whole-mount *in situ* hybridization is available and described in detail on the GUDMAP gene expression database (http://www.gudmap.org/Research/Protocols/Little.html). In brief, whole-mount *in situ* hybridization was performed by using the BioLane HTI robot with digoxigenin-labeled antisense riboprobes. Tissues were rehydrated by a series of methanol/PBTX washes, followed by a short digestion of Proteinase K, and refixed by 0.2% gluteraldehyde/4% PFA before incubation in pre-hybridization solution at 65 °C for 2 h. Tissues were later transferred into pre-hybridization solution containing 0.2 µg/ml of riboprobe, incubated at 65 °C overnight. Following post-hybridization washes, a 2-h incubation in pre-block solution followed by incubation in pre-adsorbed anti-DIG/pre-block solution was performed. After the post-antibody washes, to detect the hybridized alkaline phosphatase activity, chromogenic substrates NBT/BCIP were used. Time for color development varies between 15 min and up to 300 min depending on the specificity of the riboprobe. Once the tissue has reached its optimal intensity, the tissues were washed with 1% Triton X-100/PBS at 4 °C for a duration up to 2 days, later fixed with 4% PFA and stored in PBS at 4 °C. All whole-mount tissues were photographed manually on a 1.5% agarose gel dish, using Nikon SMZ1500 stereomicroscope system with a Nikon DXM1200f, 12-megapixel digital camera, ACT-2U Image Application Software, and Adobe Photoshop CS2. For imaging of bisected genital tubercles, this region

was dissected away from the rest of the lower urinary tissues in PBS on a Petri dish, and each sample was bisected either longitudinally or transversely with the aid of a 30G needle and number 11 surgical blade.

*Pseudo-colored gene expression overlays*

To compare multiple gene expression domains, Adobe Photoshop CS2 software was used to produce pseudo-colored gene expression images of overlaid, stage-matched tubercles at 13.5 dpc. Experimental image data were first outlined to obtain the structural outer edge of the tubercle and inverted to produce a black and white image. These were then aligned with up to two other genes using the RGB image format.

## Results

Tissue was collected for RNA extraction from E13 urethra and bladder in which the epithelial and mesenchymal layers were separated from each other using trypsin digestion or EDTA treatment, respectively (Fig. 1A). Tissue was also collected from E14 lower urinary tract (LUT) microdissected into bladder, urogenital sinus (UGS; includes the junction between the urethra, bladder, and ureters), urethra, and GT as illustrated in Fig. 1B. All data have been submitted to GEO and are available from the GUDMAP database (www.gudmap.org), from which the expression level of all genes present on the microarray can be queried individually.

*Creation of an overall view of differential gene expression across the developing lower urinary tract*

In order to identify sets of genes that are either highly expressed or comparatively over-expressed in one or more of the sampled individual LUT/GT compartments during development, probe sets were first filtered to identify those genes expressed at least at the 40th percentile of raw RMA normalized intensity in at least two replicates of each sample type. From these, probes that exhibited the highest ranked relative expression as compared to the globally referenced data set were identified, i.e., their having normalized expression in the top 2% per each of the LUT sample types (~250–400 probe sets per each of the 8 compartments). The combination of all these probe sets were hierarchically clustered and Fig. 1C shows a heat map of these 1420 probe sets across all compartments. These are presented after hierarchical clustering to display the most highly expressed genes across the different LUT sample types. A full gene list and heat map of the expression profiles manifested by these transcripts is provided in Supplementary Table 1. The expression of previously known compartment markers, including Tbx20 and Tbx18 in the bladder and the strong expression of Hoxd13 in all compartments, supports the accuracy of the data (Fig. 1C). To determine potential functional roles for these genes, the 1420 probe set list was enriched with public database annotations (e.g., GO, Jax Mouse, OMIM, TFBS, Drug Bank, TargetScan, MSigDB, etc.) using ToppGene (Chen et al., 2009). The results of these analyses are shown in Supplementary Table 2. This revealed expression of a large number of DNA binding transcription factors, particularly homeobox (*Hoxd13*, *Msx1*, *Six1*, *Irx3*, *Irx5*, *Msx2*, *Isl1*, *Pitx1*, *Pitx2*, *Hoxa10*, *Zfhx4*, *Dlx5*, *Zfhx3*, *Mkx*, *Satb2*, *Prrx1*, *Prrx2*, *Alx3*, *Alx1*, *Cux1*) and forkhead genes (*Foxf2*, *Foxd1*, *Foxa1*, *Foxn3*, *Foxq1*); fibronectin III (FnIII) domain encoding genes (*Ptprj*, *Ptpro*, *Flrt3*, *Flrt2*, *Cntn3*, *Dcc*, *Crlf1*, *Epha5*, *Epha4*, *Epha7*, *Robo1*), and genes encoding cell–cell adhesion molecules. The most active biological processes included cell–cell adhesion with 21/104 cadherin domain containing proteins being expressed in the developing LUT (*Pcdh10*, *Pcdh18*, *Cdh11*, *Pcdha10*, *Pcdha11*, *Pcdha13*, *Dsg2*, *Frem1*, *Dsc2*, *Pcdha6*, *Pcdha7*, *Pcdha9*, *Pcdha2*, *Pcdha3*, *Pcdha4*, *Pcdha5*, *Pcdha1*, *Pcdhb7*, *Pcdhc2*, *Pcdhac1*, *Pcdhgb2*). The most active pathways were the Wnt signaling (*Wnt5A*, *Gng4*, *Myh3*, *Pcdh10*, *Pcsh18*, *Nkd2*, *Wnt7A*, *Cdh11*, *Pcdha10*, *Pcdha11*, *Pcdha13*, *FrzB*, *Pcdha6*, *Pcdha7*, *Pcdha9*, *Pcdha2*, *Pcdha3*, *Pcdha4*, *Pcdha5*, *Pcdha1*, *Pcdhb7*, *Bcl9*, *Fzd6*, *Ankrd6*, *Wnt6*, *Myst4*, *Pcdhac2*, *Pcdhac1*, *Axin2*, *Lef1*, *Pcdhgb2*, *Dkk2*, *Dkk1*, *Dkk3*, *Axin2*, *Wif1*, *Nfat5*), hedgehog signaling (*Shh*, *Bmp5*, *Gli3*, *Wnt6*, *Wnt5A*, *Wnt7A*), and cadherin signaling pathways. ToppGene analysis identified many genes involved in limb/face/appendage and skeletal development. In addition, there were many genes previously implicated in neural development and ectodermal/epidermal/epithelial development gene networks, notably cadherins, collagens, and keratins. Examining the data for genes linked to human or mouse phenotypes involving the urogenital tract revealed genes known to be critical for reproductive, genital, bladder/ureter, and kidney development. This set of genes overlapped genes involved in anal development, presumably reflecting the common origin of the bladder and urethra from the cloaca, and body wall development. The strongest associations were seen between genes affecting external genitalia/reproductive tract, anal canal and body wall development (*TP63*, *Sall1*, *Sall4*, *Gli3*, *Pitx2*, *Tbx3*; Fig. 1E, Supplementary Table 3). *Sall1* and *p63* are involved in the development of all of these organs/tissues; *Sall4* is involved in all but body wall; and *Six1* is involved in body wall, kidney, and ureter development (Supplementary Table 3).

*Defining the most active networks in each compartment*

In Fig. 1C there is both considerable overlap of gene expression between all compartments of the LUT as well as clusters of gene expression more active in specific compartments. Heat maps for each compartment are presented in Supplementary Fig. 1 and complete gene lists for each compartment in Supplementary Table 1. To understand the major processes occurring in each compartment, ToppGene analysis of each compartment was performed to identify the most represented molecular functions, biological processes, cellular components, protein domains, pathways, and phenotypes. A summary of this analysis is presented in Table 2. A complete analysis of gene ontology for each compartment-enriched gene set is presented in Supplementary Table 2. This analysis reinforced the prevalence of cadherin and Wnt signaling, the predominance of transcription factor activity, and the association of LUT compartments with genes involved in appendage, skeletal, neural, epithelial, and urogenital development. Cluster analysis suggested strong alignment between E13 bladder epithelium and E13 urethra epithelium, but less of a relationship between the bladder and urethral mesenchyme of the same time point (Fig. 1D). E13 bladder mesenchyme was most similar to E14 total bladder due to the expression of muscle genes (*Tnnt2*, *Kcnq5*, *Actg2*, *Myh11*). These two bladder samples were also outliers in their lack of association with cadherin or Wnt signaling. E14 UGS and urethra clustered together, whereas GT was distinct aside from a cluster of genes co-expressed in E13 urethra mesenchyme (*Fgf9*, *Alx3*, *Foxd1*, *Msx1*, *Wnt5a*). These genes have all previously been reported in GT development, reflecting the fact that the E13 urethra sample would have included GT. E13 urethral mesenchyme and UGS showed significant overlap (*Myrip*, *Mapk10*, *Prph*, *Phox2b*, *Sthm2*, *Sthm2*, *Gdap1*) with enrichment for genes involved in neurogenesis and neural crest, including the GDNF/Ret pathway (*Gfra1*, *Gfra2*).

*LUT compartment-enriched gene expression highlights innervation and vascularization*

The expression profiling was then reanalyzed so as to specifically identify differences in gene expression between the compartments being assessed. The intention of identifying compartment-enriched genes was to identify unique markers of each compartment. Supplementary Table 4 lists all genes displaying compartment-

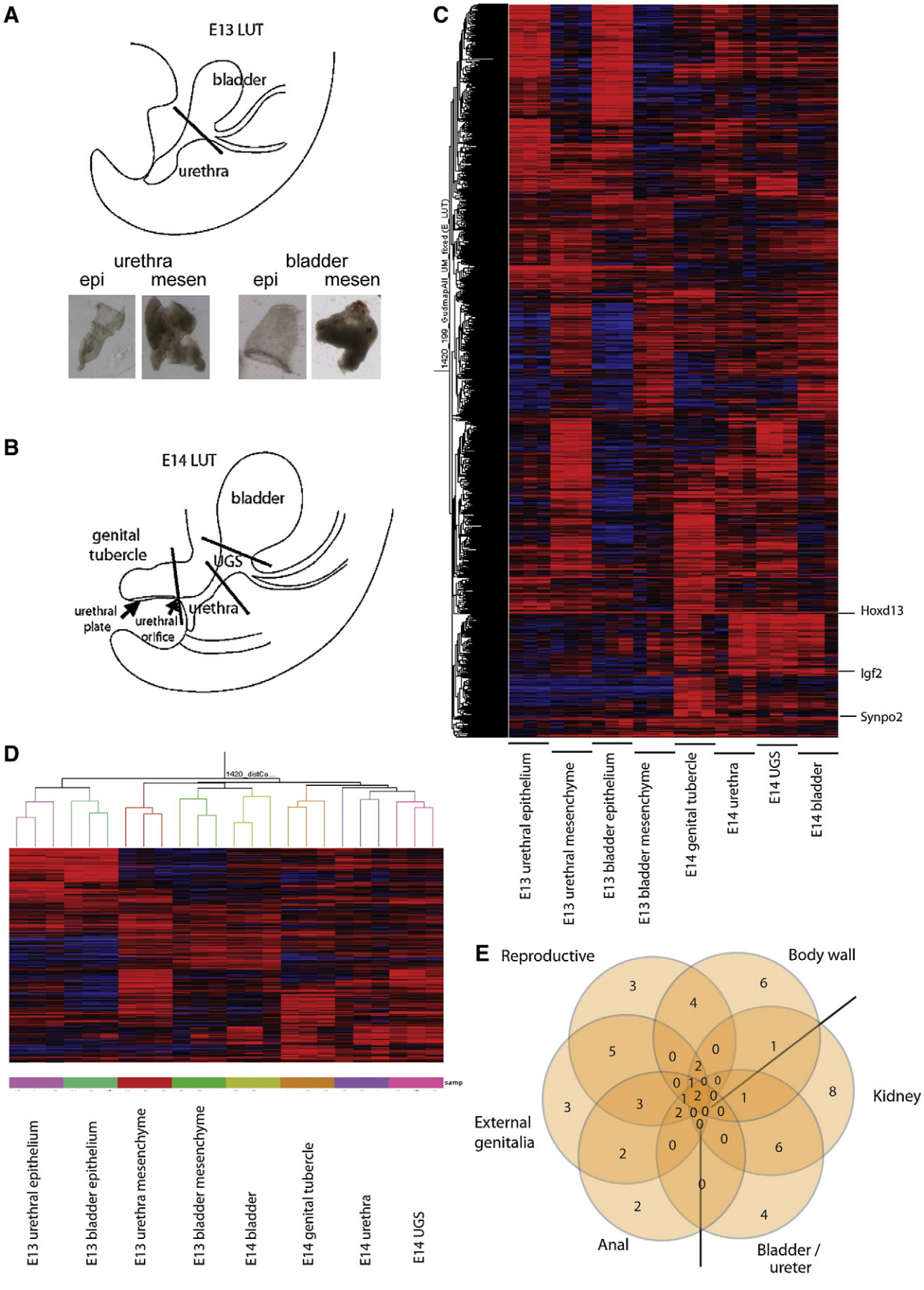
A
E13 LUT
bladder
urethra
urethra
epi
mesen
bladder
epi
mesen
B
E14 LUT
bladder
genital tubercle
UGS
urethral plate
urethral orifice
urethra
C
Hoxd13
Igf2
Synpo2
E13 urethral epithelium
E13 urethral mesenchyme
E13 bladder epithelium
E13 bladder mesenchyme
E14 genital tubercle
E14 urethra
E14 UGS
E14 bladder
D
E13 urethral epithelium
E13 bladder epithelium
E13 urethra mesenchyme
E13 bladder mesenchyme
E14 bladder
E14 genital tubercle
E14 urethra
E14 UGS
E
Reproductive
Body wall
Kidney
External genitalia
Anal
Bladder / ureter

enriched expression for each compartment. Fig. 2 shows a heat map highlighting gene clusters with urethra-enriched or GT-enriched gene expression. Within the heat map, it is possible to identify E14 urethra-enriched genes that are likely to mark epithelium versus mesenchyme by examining their co-expression in E13 urethra and bladder epithelium. Whole-mount *in situ* hybridization (WISH) was used to validate enrichment of gene expression in each compartment. Riboprobes were generated for a total of 94 genes (Supplementary Table 5) and all WISH results were fully annotated for gene expression and submitted to the Genitourinary Development Molecular Anatomy Project website (www.gudmap.org; McMahon et al., 2008) and riboprobe sequences are shown in Supplementary Table 5. WISH was performed on E13.5 embryos for 11 urethra-specific genes (Fig. 3C), including *Irs4* and *2310076G05Rik*, seventeen E14 UGS-enriched genes, including *Elavl4*, *Gap43*, and *Ascl1* (Fig. 3D), and eight E14 bladder-enriched genes, including *Maf* and *Klhl4* (Fig. 3E). Quite a number of UGS-enriched genes were expressed in the pelvic ganglia. Bladder-enriched genes highlighted bladder innervation and vasculature as well as markers specific to the dome of the bladder (Fig. 3E). Schematic representations of these regions of the LUT are shown in Fig. 3A and B.

### *Analysis of androgen-independent genital tubercle development*

To validate the utility of the data set, we focused on the gene expression observed in the E14 GT given that this was the most unique set of compartment-enriched sets. As previous studies have reported expression of genes from within the BMP, FGF, Wnt, and hedgehog pathways in GT development, we examined the expression of all members of these pathways present on the Affymetrix chips (Supplementary Table 6). This confirmed the expression of many pathway members known to be expressed in the GT although, as expected, few of these genes showed GT-enriched or -specific gene expression. Genes from the FGF/Hedgehog/Wnt pathways showing expression in E13 LUT and E14 GT included *Fgf9* (mesenchyme), *Pik3ca*, *Npc1*, *Fgfr3*, *Fgfbp1*, *Wnt4*, *Wnt5a*, *Wnt7a*, *Wnt7b*, and *Wnt10a*. A smaller number of genes from the BMP pathway showed expression in the E13 LUT and E14 GT, including *Bmp2*, *Bmp4*, *Bmp7*, *Fstl1*, and *Gsk3b*. *Bmp5* showed GT-restricted gene expression at E14, but expression levels were low. The genes selected as being GT-enriched were analyzed for pathway, disease, or GO term associations (Supplementary Table 7). As for the analysis of the most active pathways in this compartment, this revealed a strong link to Wnt pathway signaling. It also reinforced the previously proposed association between GT-enriched genes and genes involved in limb and craniofacial development (Supplementary Tables 2 and 7; Table 1).

WISH of E13.5 GT was performed to validate the microarray data and investigate the spatial relationship of the GT epithelial-enriched ("on" in GT and E13 urethral epithelium), GT mesenchyme-enriched ("on" in GT and E13 urethral mesenchyme), and GT-specific genes (only observed in E14 GT). As GT was not separated from LUT at E13, genes expressed in E13 urethral epithelium or mesenchyme, but not expressed in E14 urethra, were likely to represent early GT genes, possibly enriched for those expressed along the urethral plate. Those restricted to the epithelium at E13 were most likely to be expressed in the epithelium of urethral plate of the E14 GT, while those expressed in the mesenchyme at E13 were likely to be in the mesenchyme along the urethral plate in the E14 GT. WISH validated these assumptions. In order to fully annotate the gene expression patterns observed, we modified the previous genitourinary tract ontology (Little et al., 2007) to increase the level of anatomical resolution for the TS21 genital tubercle (Supplementary Fig. 2). Fig. 4 demonstrates examples of GT-enriched and GT-restricted gene expression patterns. A schematic representation of the features of the developing GT can be seen at http://www.gudmap.org/Organ_Summaries/index.html (genital tubercle of male and female). In total, validation of GT-enriched or restricted expression was observed for 43/58 genes examined by WISH (74% validation of array data). Table 2 summarizes the annotated expression patterns of these genes in the developing GT. For those where validation was not observed, signal was either absent/very weak or expression was seen in additional sites. The former is likely to result from the reduced sensitivity of the ISH in comparison to microarray (negatives). The latter may result from the riboprobe detecting an isoform of the gene not identified by the Affymetrix oligonucleotide (additional sites of expression).

### *Novel gene expression domains on the dorsal surface of the presumptive glans*

The dorsal side of the extending genital tubercle is longer than the ventral surface such that there is an overhanging dorsal lip and the orifice of the DUE is on the ventral side. At E13.5, there is a discernable glans that is most prominent from the dorsal side. Analysis of the gene expression patterns seen in E13.5 GT revealed some distinct patterns of expression as yet unreported. Of particular interest were very tightly delineated domains of expression on the dorsal surface of the genital tubercle. These genes did not show dorsally restricted expression but did reveal specific dorsal patterns of expression around the tip of the extending glans that allowed the subdivision of distal genital tubercle into a number of expression patterns not previously reported. *Dlx6os1*, *Cpm*, *Mup1*, *Sty13*, and *Hs3st3b1* each showed distinct but non-overlapping expression in specific regions of the distal GT (some epithelial, some mesenchymal) other than the DUE (Figs. 4 and 6; www.gudmap.org). Distinct gene expression patterns were also seen on the preputial swellings (e.g., *Sostdc1*, *Dsc3*, Fig. 4) and preputial glands (e.g., Gja1, Fig. 4).

### *Validation of Wnt5a signaling in GT mesenchyme and identification of an associated gene network*

The WISH-confirmed GT-enriched genes contained many Wnt signaling pathway members (see Supplementary Fig. 3). As previously reported, *Wnt5a* was expressed in the mesenchyme of the distal genital tubercle (Yamaguchi et al., 1999; Suzuki et al., 2003; Fig. 5A). In order to predict genes interacting with Wnt5a within this compartment, we generated pseudo-colored overlays of WISH results from all GT-enriched genes. This allowed the direct alignment of up to three genes to examine in detail their spatial relationships (Fig. 5B). *Wnt5a* expression overlapped with the distal GT mesenchymal expression of Frizzled b (*Frzb*), a secreted frizzled protein that acts as an inhibitor of the pathway (Fig. 5Bc, c′). The proximal edges of the *Wnt5a* expression domain were also marked by a unique and distinct expression pattern of *Dkk1*, an inhibitor of canonical Wnt signaling (Fig. 5Bb–e, b′–e′). This combination of ligand and inhibitor appears to delineate the GT equivalent of a progress zone in the glans/distal GT. Comparison of this domain of expression with other genes suggests a possible interaction with several other genes

**Fig. 1.** Defining the gene expression profile of the developing lower urinary tract. (A) Diagram of the E13 LUT indicating the point of dissection to separate E13 urethra from E13 bladder and the resultant separation of epithelium from mesenchyme achieved using trypsin digestion and EDTA dissociation, respectively. (B) Diagram of the E14 LUT indicating the point of dissection to delineate four spatial regions; genital tubercle (GT), urethra, UGS, and bladder. (C) Heat map of the 1420 most highly expressed genes across all eight compartments of the developing LUT. (D) Cluster diagram highlighting the hierarchical relationships between all samples analyzed (eight compartments in triplicate). Note that all replicates correctly clustered with their compartment of origin. (E) Venn diagram indicating the degree of gene overlap between the processes of reproductive, external genital, anal, body wall, kidney, and bladder/ureter development identified in the GT data set.

**Table 2**
Observed gene expression patterns for genital tubercle-enriched genes. Affy ID, Affymetrix ID; DGTE, distal genital tubercle epithelium; DGTM, distal genital tubercle mesenchyme; DUE, distal urethral epithelium; PUE, proximal urethral epithelium; UPM, mesenchyme underlying the urethral plate; PPSM, preputial swelling mesenchyme; PPSE, preputial swelling epithelium; PPG, preputial gland.

| Symbol | Cluster | Affy ID | Distal GT | | Urethral epithelium | | UPM | Preputial swelling | | |
|---|---|---|---|---|---|---|---|---|---|---|
| | | | DGTM | DGTE | DUE | PUE | | PPSM | PPSE | PPG |
| Col17a1 | GT epithelium -enriched | 1418799_a_at | – | + | + | – | – | – | + | – |
| Gjb2 | GT epithelium-enriched | 1423271_at | – | + | – | – | – | – | + | – |
| Krt2-6a | GT epithelium-enriched | 1422784_at | – | – | + | + | – | – | – | – |
| Krt2-5 | GT epithelium-enriched | 1424096_at | – | + | + | + | – | – | + | – |
| Dlx5 | GT epithelium-enriched | 1449863_a_at | + | – | – | – | + | – | – | – |
| Dsc3 | GT epithelium-enriched | 1434534_at | + | + | + | – | – | – | + | – |
| Wnt7a | GT epithelium-enriched | 1423367_at | – | + | + | + | – | – | + | – |
| Serpinb3b | GT epithelium-enriched | 1422940_x_at | + | – | – | + | + | – | – | – |
| Cxcl14 | GT epithelium-enriched | 1418457_at | – | + | + | – | – | – | + | – |
| Shox2 | GT mesenchyme-enriched | 1438042_at | – | – | – | – | – | + | – | – |
| Lef1 | GT mesenchyme-enriched | 1454734_at | + | – | – | – | + | + | – | + |
| Syt13 | GT mesenchyme-enriched | 1434470_at | + | – | – | – | – | – | – | – |
| Prdm1 | GT mesenchyme-enriched | 1420425_at | + | – | – | – | + | + | – | – |
| Dkk1 | GT mesenchyme-enriched | 1420360_at | + | – | + | – | + | – | – | – |
| Tcfap2b | GT mesenchyme-enriched | 1435670_at | + | – | – | – | + | – | + | – |
| Hs3st3b1 | GT mesenchyme-enriched | 1433977_at | + | – | – | – | + | + | – | – |
| Wnt5a | GT mesenchyme-enriched | 1436791_at | + | – | + | – | + | – | – | – |
| Kcnab1 | GT mesenchyme-enriched | 1448468_a_at | + | – | – | – | + | + | – | – |
| Apcdd1 | GT mesenchyme-enriched | 1449070_x_at | + | – | – | – | + | + | – | – |
| | GT mesenchyme-enriched | 1440630_at | + | – | – | + | + | – | – | – |
| Unc5d | GT mesenchyme-enriched | 1440484_at | + | – | – | + | + | – | – | – |
| Kcna4 | GT mesenchyme-enriched | 1438613_at | + | – | – | + | – | + | – | – |
| D930002L09Rik | GT mesenchyme-enriched | 1444452_at | + | – | – | + | – | – | – | – |
| Satb2 | GT mesenchyme-enriched | 1427017_at | + | – | – | + | + | – | – | – |
| Frzb | GT mesenchyme-enriched | 1416658_at | + | – | – | – | + | – | – | – |
| Mup1 | E14 GT restricted | 1420465_s_at | + | – | – | – | – | – | – | – |
| Dlx6os1 | E14 GT restricted | 1438799_at | + | – | – | – | + | – | – | – |
| Trpm1 | E14 GT restricted | 1437445_at | + | – | – | – | – | – | – | – |
| Msx1 | E14 GT restricted | 1448601_s_at | + | – | – | – | + | – | – | – |
| Col19a1 | E14 GT restricted | 1456953_at | + | – | – | + | + | – | – | – |
| Col19a1 | E14 GT restricted | 1421698_a_at | + | – | – | + | + | – | – | – |
| Ptgfr | E14 GT restricted | 1420349_at | + | – | – | + | + | – | – | – |
| | E14 GT restricted | 1445804_at | + | – | – | + | + | – | – | – |
| Tle4 | E14 GT restricted | 1430384_at | – | – | – | + | – | – | – | – |
| Dlx6os2 | E14 GT restricted | 1440797_at | + | – | – | + | + | – | – | – |
| Sostdc1 | E14 GT restricted | 1449340_at | – | + | + | – | – | – | + | – |
| Wif1 | E13 urethra and GT | 1425425_a_at | + | – | – | – | + | + | – | – |
| Dlx1 | E13 urethra and GT | 1449470_at | – | + | + | – | + | – | – | – |
| Gja1 | E13 urethra and GT | 1415801_at | + | – | + | – | + | + | – | + |
| Osr2 | E13 urethra and GT | 1426155_a_at | + | – | – | – | + | + | – | – |
| Msx2 | E13 bladder and GT | 1449559_at | + | + | + | – | + | – | – | – |
| Tcfap2c | E13 bladder and GT | 1448977_at | + | – | – | – | + | – | – | + |
| Cpm | E13 bladder and GT | 1429413_at | + | – | + | – | + | – | – | – |

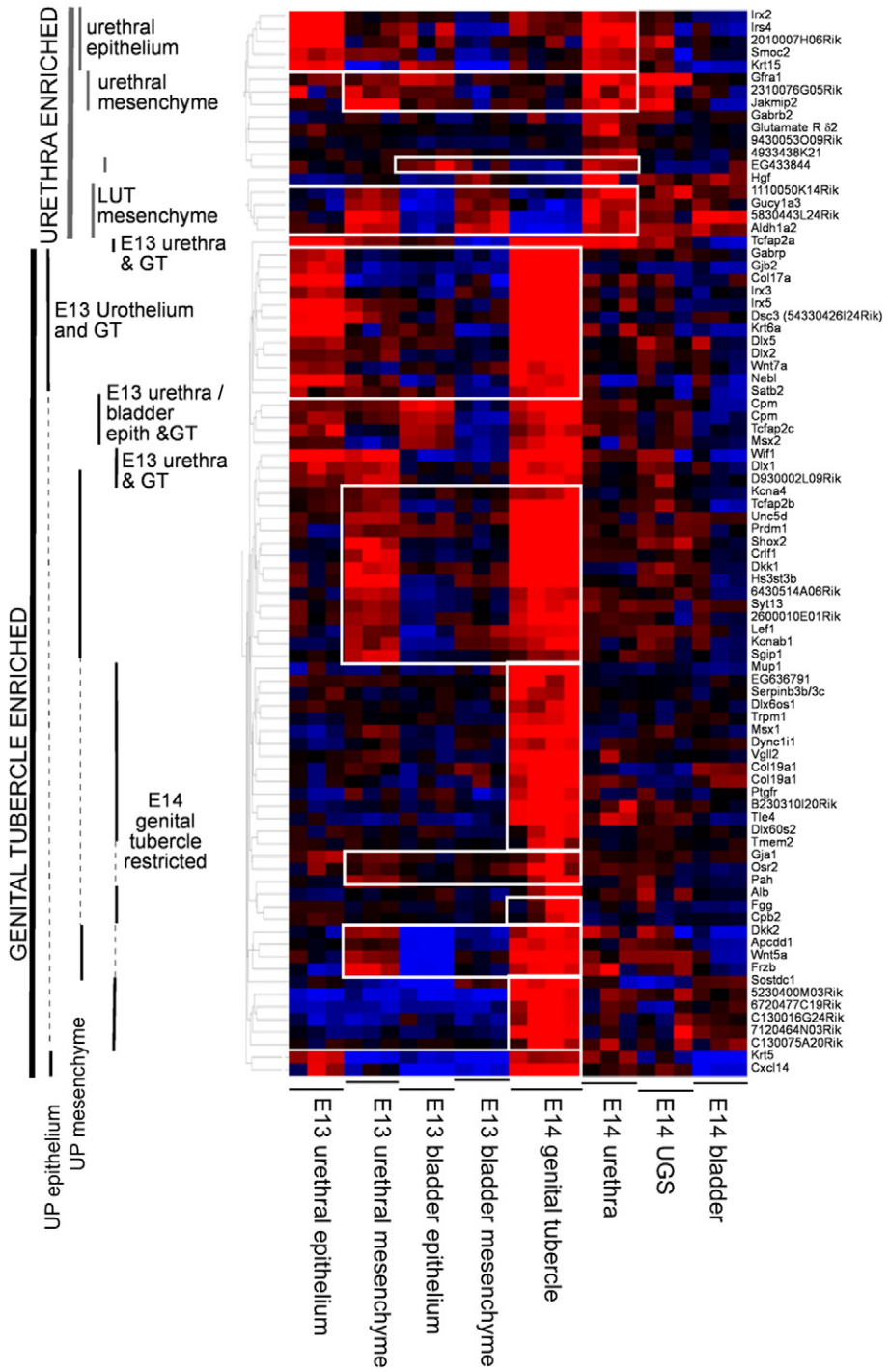


**Fig. 2.** Heat map of gene expression across E14 urethral-enriched and genital tubercle-enriched genes. Urethral-enriched genes can be subdivided into epithelial versus mesenchymal based on the expression in E13 urethra. Genital tubercle-enriched genes were subdivided into urethral plate (UP) epithelium (expressed in genital tubercle and E13 urethral plate epithelium but not E14 urethra), UP mesenchyme (expressed in genital tubercle and E13 urethral mesenchyme but not E14 urethra), and genital tubercle-specific genes (expressed only in GT).

from within the GT mesenchyme-enriched cluster. *Kcnab1* shows overlapping expression with Wnt5a in the glans but is expressed in a wider region of the GT mesenchyme, notably not overlapping the expression of *Dkk1* (Fig. 5Bd, d′). The Wnt downstream signaling molecule *Lef1* also shows partial synexpression with *Wnt5a* (Fig. 5Bb, b′). In contrast, the short stature homeobox 2 gene (*Shox2*) shows a complementary pattern of expression (Fig. 5Be, e′). These visual comparisons of spatial expression patterns suggest an interaction between these genes. To both validate these predictions and define potentially Wnt5a-interacting genes, the initial GT-enriched data set was reanalyzed to seek genes displaying synexpression across the LUT/GT with *Wnt5a* using *K*-means and hierarchical clustering. This identified a cluster of genes with moderate to high expression in the E13 urethral mesenchyme (*Wnt5a*, *Dkk2*, *Frzb*, *Wif1*, *Lef1*, *Phex*, *Runx2*, *Dlx2*, *Msx1*, *Dlx1*, *Shox1*, *Satb2*, *Osr2*, *Runx5*, *Cacna2d3*, *Prdm1*, *Kcnab1*, *Tfap2b*, *Nkx1.2*, *Kcna4*). ToppGene analysis of this cluster identified enrichment for genes involved in skeletal and cartilage development/morphology (Fig. 5C). For example, *Runx2* has

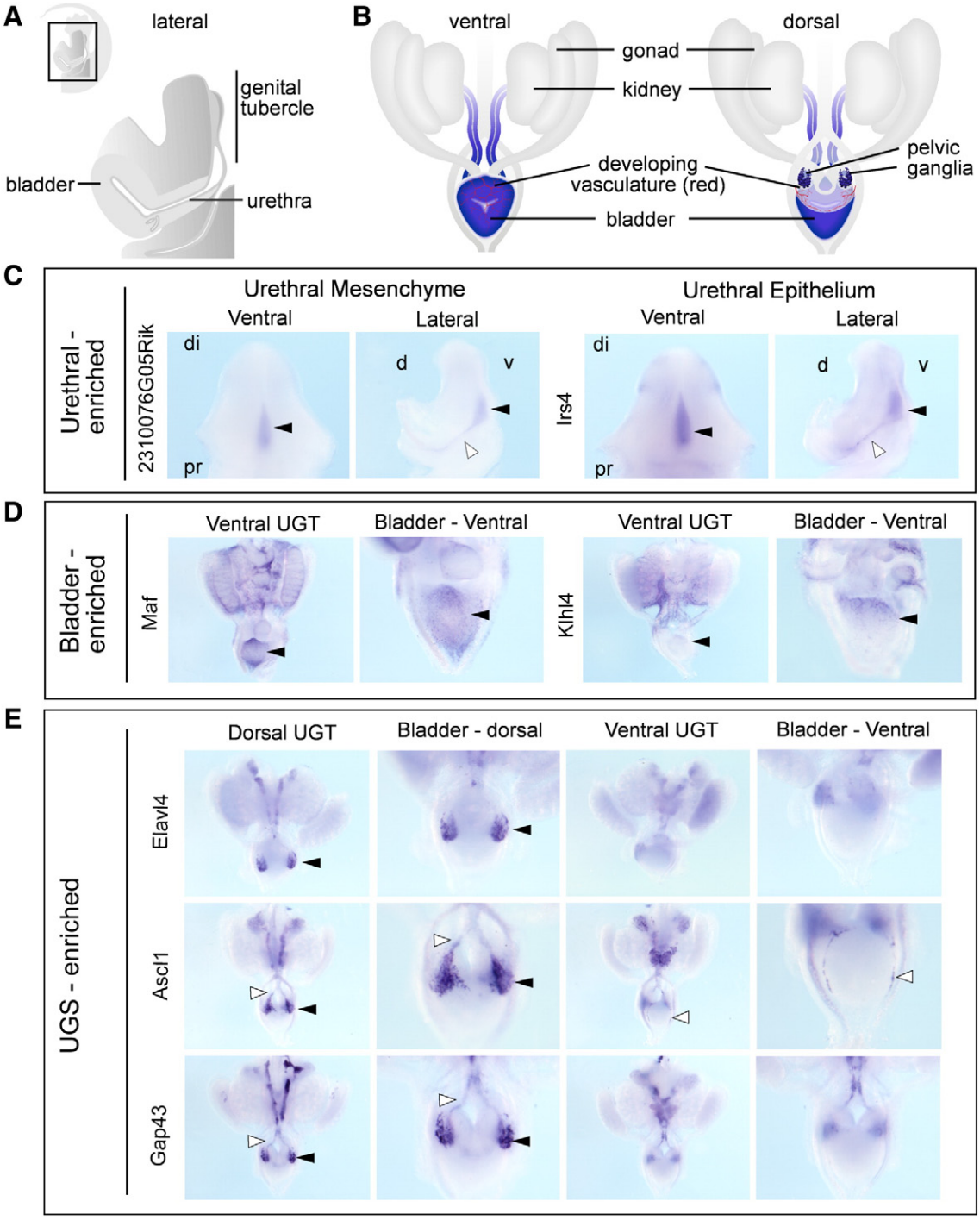


**Fig. 3.** Validation of E14 urethral, bladder, and UGS-enriched genes. (A) Schematic diagram of a bisected LUT/GT, lateral view, illustrating the bladder, UGS, and urethra. UP, urethral plate; DUE, distal urethral epithelium. (B) Schematic diagram of whole urogenital tracts, ventral and dorsal views. (C) Urethral-enriched genes with epithelial (*Irs4*) and mesenchymal (*2310076G05Rik*) expressions displayed as ventral (left) and lateral (right) views. Expression can be seen along the UP (solid arrowheads) and in the urethra itself (open arrowheads). (D) E13 bladder-enriched genes *Maf* and *Klhl4* showing expression in vasculature and differential expression in the dome of the bladder (solid arrowheads, rostral end). (E) UGS-enriched genes *Elav4*, *Ascl1*, and *Gap43* revealing specific expression in migrating neural crest cells (open arrowheads) and developing ganglia (solid arrowheads) at the base of the dorsal surface of the bladder. di, distal; pr, proximal; d, dorsal; v, ventral.

previously been shown to be regulated by *Shox2* in limb chondrogenesis prior to long bone formation (Cobb et al., 2006). These genes often displayed differential anterior–posterior limb and dorsal–ventral GT expression, reinforcing congruence in the development of these two appendicular structures. Many also showed differential proximal–distal patterning in both structures, as is the case for

**Fig. 4.** Validation of E14 genital tubercle-enriched gene expression. (A) Genital tubercle-enriched genes predicted to be expressed in UP epithelium and GT (*Col17a*, *Gja1*, *Dsc3*) or UP mesenchyme and GT (*Syt13*, *Kcnab1*, *Osr2*). Expression can also be seen in preputial gland (*Gja1*), distal urethral epithelium (*Col17a*, *Gja1*, *Dsc3*), surface epithelium of glans and preputial swelling (*Col17a*, *Gja1*, *Dsc3*) and preputial swelling mesenchyme (*Kcnab1*, *Osr2*). (B) Genital tubercle-restricted genes (*Dlx6os1*, *Sostdc1*, *Cxcl14*) showed expression in preputial swelling epithelium (*Sostdc1*, *Cxcl14*), distinct domains across the dorsal GT (*Dlx6os1*, *Sostdc1*, *Cxcl14*), and distal genital tubercle (glans; *Dlx6os1*). Material is presented from left to right as whole mounts of ventral GT, lateral GT (dorsal to the left side), dorsal GT, and transverse and longitudinal sections through whole-mount specimens. di, distal; pr, proximal; d, dorsal; v, ventral; DUE, distal urethral epithelium; UP, urethral plate; UPE, UP epithelium; UPM, UP mesenchyme; PPG, preputial gland; PPS, preputial swelling.

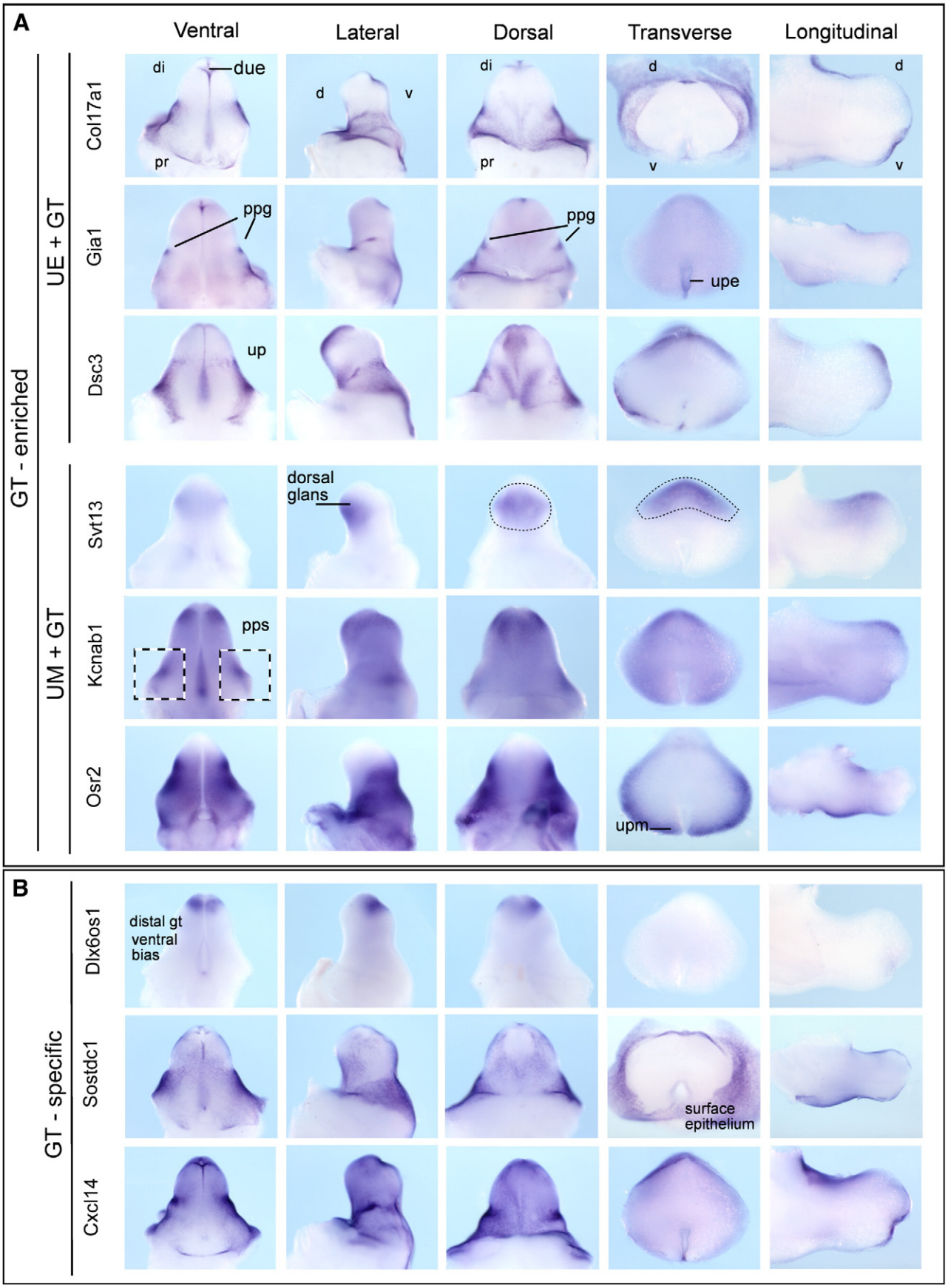
A
Ventral
Lateral
Dorsal
Transverse
Longitudinal
GT - enriched
UE + GT
UM + GT
Col17a1
Gia1
Dsc3
Svt13
Kcnab1
Osr2
di
due
pr
d
v
ppg
up
upe
dorsal glans
pps
upm
B
GT - specific
Dlx6os1
Sostdc1
Cxcl14
distal gt ventral bias
surface epithelium

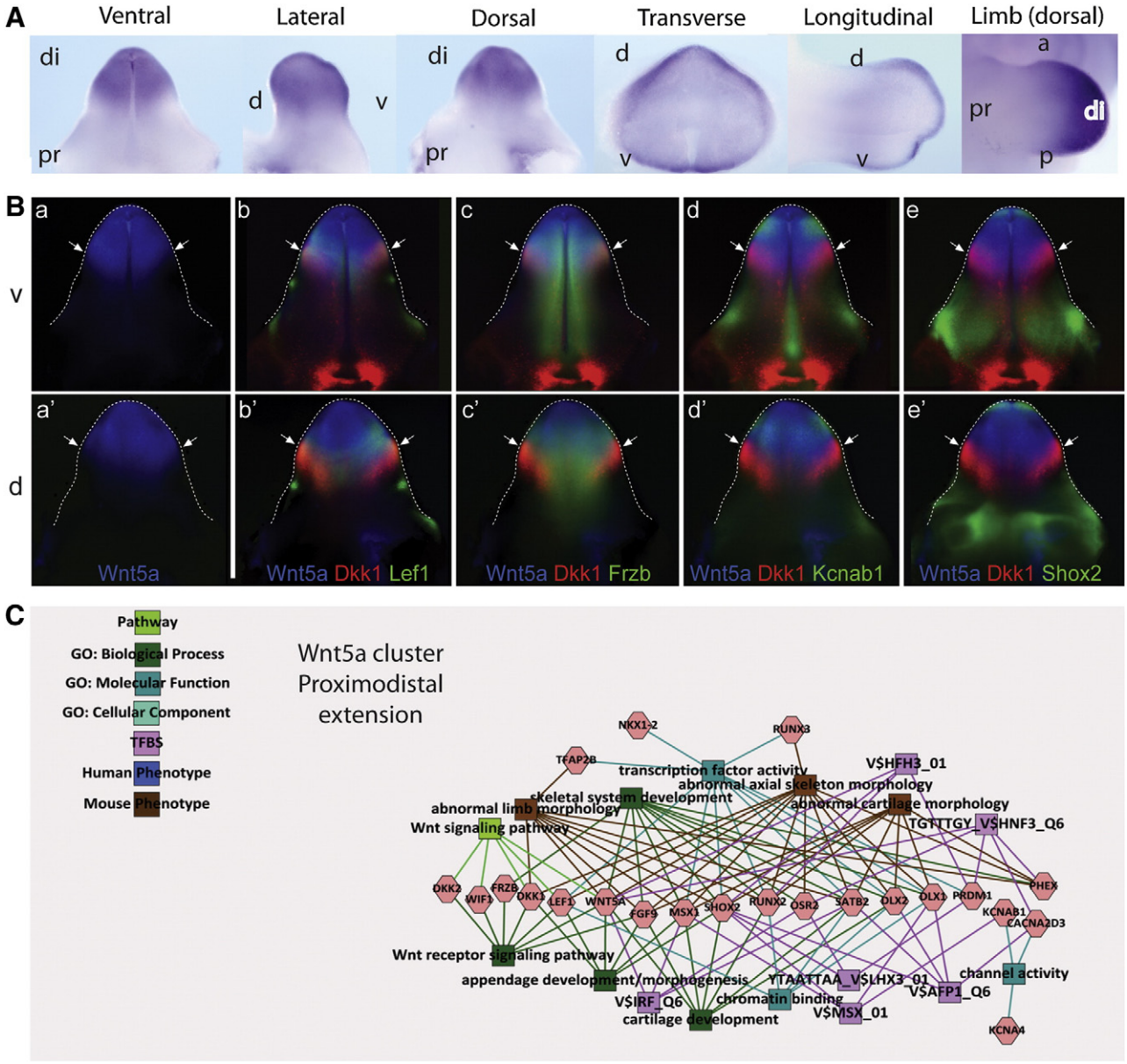


**Fig. 5.** Identification of Wnt5a associated gene networks in GT development. (A) Whole-mount ISH of Wnt5a in the developing E13.5 GT showing ventral, lateral, dorsal, transverse, and longitudinal views, as well as Wnt5a expression in the limb (dorsal view). di, distal; pr, proximal; d, dorsal; v, ventral; a, anterior; p, posterior. (B) Pseudo-colored expression pattern overlays of known and candidate genes of a *Wnt5a* network. Experimental WISH images of stage-matched genital tubercles at 13.5 dpc were pseudo-colored and overlaid with either *Wnt5a* (a–e, a′–e′). Ventral (v; a–e) and dorsal (d; a′–e′) views are shown and the edge of the GT is outlined with a dotted line. *Wnt5a* network genes include (a, a′) *Wnt5a* alone, (b, b′) *Wnt5a*/*Dkk1*/*Lef1*, (c, c′) *Wnt5a*/*Dkk1*/*Frzb*, (d, d′) *Wnt5a*/*Dkk1*/*Kcnab1*, and (e, e′) *Wnt5a*/*Dkk1*/*Shox2*. Arrows indicate the border of the *Wnt5a* distal GT expression domain. All genes showed some degree of overlap with the *Wnt5a* domain. *Dkk1* showed overlapping expression with (b, b′) *Lef1* and (c, c′) *Frzb*, in contrast to (d, d′) *Kcnab1* and (e, e′) *Shox2*, which did not overlap with the distal *Dkk1* domain. (C) GT mesenchyme-enriched gene cluster associated via hierarchical clustering decorated with GO terms and known transcription factor binding sites and known human and mouse phenotype associations. This cluster shows strong links to limb morphogenesis, particularly of mesodermal elements including cartilage and bone.

Wnt5a. This suggests possible interactions between these genes in proximal–distal extension of the GT.

*Evidence for a Wnt7a-associated gene network in the epidermis of the GT*

In contrast to Wnt5a, *Wnt7a* was expressed in the surface epithelium of the GT with stronger expression on the dorsal surface (Fig. 6A). Little attention has been paid to expression in the dorsal GT. Wnt7a was also expressed on the surface epithelium of the preputial swellings (Fig. 6A). Pseudo-colored overlays suggested co-expression of Wnt7a, the BMP antagonist sclerostin domain containing-1 (*Sostdc1*) and keratin 2–5 (*Krt5*) in tightly defined regions of the dorsal epithelial layer of the GT. Expression of these genes was also seen in the preputial swellings, but these genes were excluded from the dorsal distal glans other than at the DUE (Fig. 6Bcd). Also epithelial in expression were several genes with complementary expression patterns on the dorsal distal glans. These included desmocollin 3 (*Dsc3*; Fig. 6Bb) and *Gjb2* (Fig. 4), both genes previously associated with skin development. *K*-means and hierarchical clustering supported the association of these and other genes as representing a synexpression group in E13 urethral epithelium, therefore potentially restricted to surface epithelium (*Wnt7a*, *Dlx5*, *Msx2*, *Tfap2c*, *Krt2-5*, *Gja1*, *Irx3*, *Irx5*, *Tfap2a*, *Gabrp*, *Krt6a*, *Krt14*, *Col17a*, *Dsc3*, and *Pkp1*).

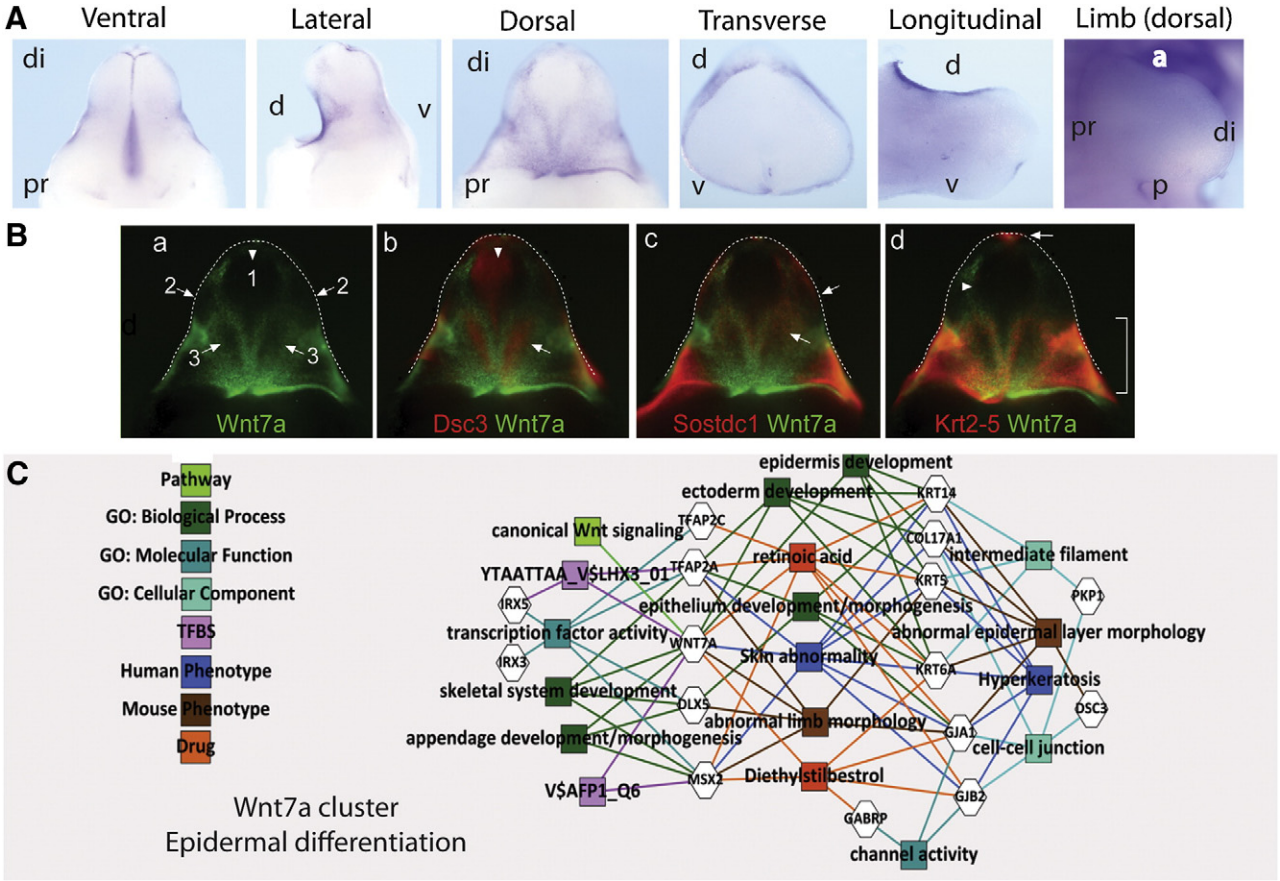


**Fig. 6.** Identification of Wnt7a associated gene networks in GT development. (A) Whole-mount ISH of Wnt7a in the developing E13.5 GT showing ventral, lateral, dorsal, transverse, and longitudinal views, as well as Wnt5a expression in the limb (dorsal view). (B) Pseudo-colored expression pattern overlays of known and candidate genes of a *Wnt7a* network. Experimental WISH images of stage-matched genital tubercles at 13.5 dpc were pseudo-colored and overlaid with (a–d) *Wnt7a*. Dorsal (d; a–d) views are shown and the edge of the GT is outlined with a dotted line. *Wnt7a* network genes include (a) *Wnt7a* alone, (b) *Dsc3*/*Wnt7a*, (c) *Sostdc1*/*Wnt7a*, and (d) *Krt5*/*Wnt7a*. (a) Arrows indicate the main regions (1–3) on the dorsal side of the GT where *Wnt7a* was not expressed. (b) *Dsc3* showed a complementary pattern to *Wnt7a* with strong, tightly restricted expression in regions 1 and 3 (arrows) but was expressed in the epithelium. (c, d) *Sostdc1* and *Krt5* showed overlapping expression with *Wnt7a*. *Sostdc1* was expressed more broadly than *Wnt7a* and extended into regions 2 and 3 (arrows), however like *Wnt7a*, expression was absent from the central region 1. (d) *Krt5* expression closely resembled *Wnt7a* with strong expression in the proximal *Wnt7a* domains. In the distal *Wnt7a* domains, only weak *Krt5* expression was seen (arrowhead), except for a small region of strong expression at the distal GT tip (arrow). (C) GT epithelium-enriched gene cluster associated via hierarchical clustering decorated with GO terms and known transcription factor binding sites and known human and mouse phenotype associations. This cluster shows strong links to retinoic acid and diethylstilbestrol regulation as well as epithelium and epidermal differentiation, notably in the limbs.

ToppGene analysis of this Wnt7a-associated cluster showed a strong link with epithelial and epidermis development/morphology, including clear links to skin abnormalities (including hyperkeratosis) in humans (Fig. 6C). Genes within this cluster are involved in cell–cell junction and intermediate filament biology and some (*Gjb2*, *Dsc3*, and *Krt5*) have previously been reported to be involved in plantar–palmar expression in the developing limb, as has *Wnt7a*. Of particular note, many genes within this cluster are regulated by diethylstilbestrol (*Wnt7a*, *Msx2*, *Gja1*, *Gjb2*, *Tfap2c*, *Gabrp*, *Krt6a*) and/or retinoic acid (*Krt14*, *Krt6a*, *Wnt7a*, *Tfap2a*, *Krt5*, *Gja1*, *Gjb2*, *Tfap2c*). A final cluster of genes was identified using *K*-means and hierarchical clustering. This represented GT-specific genes, many of which showed distinct proximal–distal restriction of expression in the GT (Supplementary Fig. 4). Heat maps of each of these clusters (GT mesenchyme (Wnt5a) associated, GT epithelium (Wnt7a) associated, and GT specific) are shown in Supplementary Fig. 5.

### *A comparison of gene expression during appendage formation*

Congruence of molecular processes in appendicular outgrowth was first observed between limb and branchial arch development with the observation of a key role for Fgf8 in the patterning of the first branchial arch (Trumpp et al., 1999). As for the limb, Fgf8 expression is seen in the overlying ectoderm of the first branchial arch, which is required for the survival and migration of the underlying mesenchyme. A similar congruence was then observed for genital tubercle development (Haraguchi et al., 2000; Yamada et al., 2006) with hedgehog and Fgf signaling showing considerable similarities in all three tissues. This began to explain the coincidence of defects within these tissues in many birth defects in humans (Schneider et al., 1999). Our analysis of the sites of expression of genes within the Wnt5a associated network in the genital tubercle would support a role for this cluster in appendage outgrowth. WISH was also performed for these genes in whole embryo to examine limb and craniofacial prominence gene expression. This showed very tight concordance in spatial expression patterns between limb and GT, as previously hypothesized (Trumpp et al., 1999; Schneider et al., 1999). Supplementary Fig. 6 schematically represents this congruence in gene expression between two of these appendicular structures; limb and GT. To further examine the hypothesis that there are similarities in GT patterning with the other appendages in the embryo, we performed WISH on E10.5 and E11.5 embryos examining expression in limb, GT, and branchial arches. In total, 74% (23/31) of GT-confirmed genes showed expression in limb and 71% (22/31) showed expression in the branchial arches/craniofacial prominences (Supplementary Table 8). In almost all cases, no other strong sites of gene expression were observed, supporting the notion of congruence in

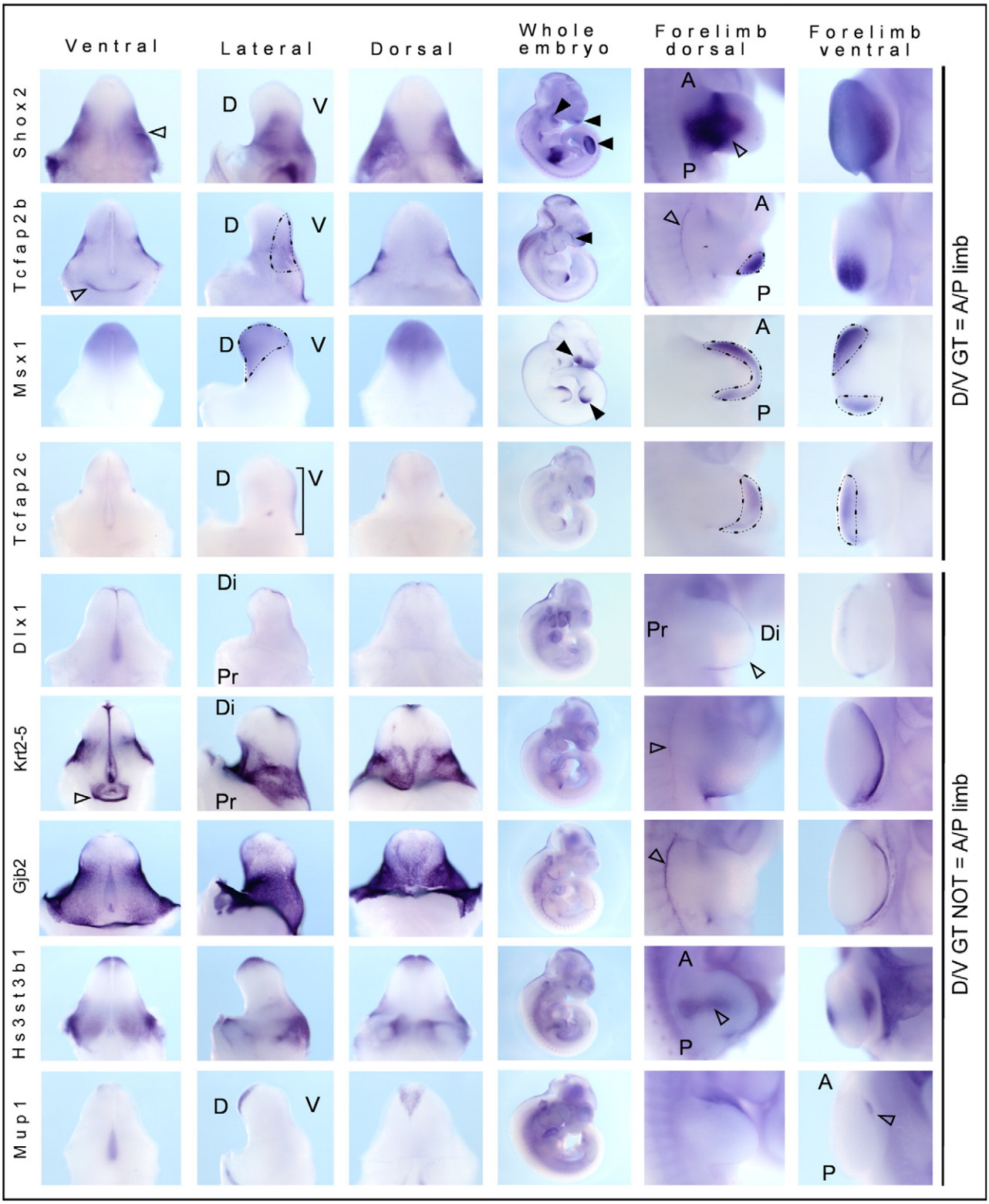


**Fig. 7.** Examination of the congruence between gene expression polarity in genital tubercle versus limb. Whole-mount ISH was performed on E13.5 genital tubercle, E10.5 whole embryo, and E10.5 forelimb. Specimens are presented from left to right as ventral GT, lateral GT, dorsal GT, E10.5 whole embryo, E11.5 dorsal limb, and apical/ventral forelimb limb views. Expression of Shox2, Tcfap2b, and Msx1 showed congruence of dorsal/ventral GT and anterior/posterior limb (lateral GT = D–V limb). Shox2 was expressed in the mesenchyme of the paired lateral preputial swellings (open arrowhead) and was also expressed in central mesenchyme of the developing limb. Tcfap2b showed preputial swelling expression. D, dorsal; V, ventral; A, anterior; P, posterior; Di, distal; Pr, proximal.

regulation of appendage development. As previously described, there was also a congruence on the axis of expression between dorsal–ventral GT and anterior–posterior limb (Fig. 7; *Shox2*, *Tfap2b*, *Msx1*, *Tfap2c*). However, a careful analysis of all GT gene expression patterns in comparison with limb expression patterns indicated that this was not always the case (Fig. 7).

## Discussion

This study describes the creation and analysis of the first comprehensive catalog of gene expression profiles describing the development of the early murine lower urinary tract and genital tubercle. Li et al. (2006) previously performed microarray analysis of GT development; however, the data presented only listed genes that increased in E16 and E17 GT versus E14. In addition, these data were collected from cDNA arrays and not Affymetrix. Hence a comparison cannot be made with these data. A comparison of these analyses with previous literature, together with our extensive whole-mount ISH analysis, supports the validity of the data. Hence, this will be a valuable resource for investigating the molecular basis of morphogenesis in this organ system and to investigate correlations between development and disease. By way of example, mutations in the renin–angiotensin system, Robo2, HNF1β (TCF2), PAX2 (renal–coloboma syndrome), EYA1 and SIX1 (branchio-oto-renal syndrome, BORS), and SALL1 (Townes–Brocks syndrome, TBS) have been reported in CAKUT patients (Weber et al., 2006). Although not previously associated with bladder, urethra, or genital defects, strong and compartment-enriched expression in the developing LUT/GT was identified for a number of these CAKUT-associated genes showed. SALL1 mutations in TBS result in renal dysplasia and VUR. Our data show that Sall1 is clearly expressed in the urethra mesenchyme and GT but not in the bladder. Only a single case report exists of a TBS patient with hypospadias (Salerno et al., 2000), but our data suggest that Sall1 may be more commonly involved in GT defects. Sall1 showed strong synexpression with Sox11, suggesting that mutations in this gene may also cause similar defects. Expression of SIX1 and EYA1, both mutated in BOR, showed highly similar gene expression patterns in the LUT. Neither was expressed in the bladder, but both were expressed in the E13 urethral mesenchyme, E14 GT, urethra, and UGS. There have been no links between these genes and genital defects, but both are associated with defects in the development of other appendages (limbs, craniofacial structures) suggesting a possible involvement in GT as well.

As a further example of the validity and potential of this data set, ToppGene analysis of the this data set also annotated six genes as being involved in anal, body wall, reproductive, and genital development (*TP63*, *Sall1*, *Gli3*, *Sall4*, *Pitx2*, *Tbx3*). Patients with anorectal malformations show high levels of genital (13.63%) or urologic (11.36%) anomalies (Saha et al., 2005), suggesting the need to carefully examine the urogenital tracts of newborns with anorectal anomalies. Nakata et al. (2009) have recently also reported an association between *Wnt5a* expression in mesenchyme close to the cloacal membrane and normal anorectal development. The link between the body wall has been less noted, although it is known that prune belly syndrome, a male-associated anomaly in the musculature of the abdominal body wall, is also associated with cryptorchidism and urinary tract anomalies (Bogart et al., 2006). Prune belly syndrome has also been linked to posterior urethral valves (Weber et al., 2005) and loci on human chromosomes 1q and 11p, as well as occurring in patients with Six1 mutations and renal defects (BOR syndrome).

To test the utility of this catalog in investigating the development of an individual compartment, we focused on the genital tubercle and have validated and fully described the spatial expression pattern of 31 genes likely to be critical for GT extension and differentiation. GT development has been proposed to be similar to the development of other appendages, including the limb and face. ToppGene analysis confirmed this suggestion although the most enriched pathway in the GT was Wnt signaling, a growth factor family known to be involved in the limb (Witte et al., 2009). In the limb, *Wnt5a* is involved in proximal–distal limb extension as loss of Wnt5a reduces proliferation within the mesenchymal progress or undifferentiated zone below the AER, resulting in limb shortening and loss of more distal structures (digits; Yamaguchi et al., 1999). This can be mimicked by inactivation of mesenchymal β-catenin (Hill et al., 2006), suggesting that this process involves canonical Wnt signaling (Geetha-Loganathan et al., 2008). The canonical Wnt inhibitor, *Dkk1*, is expressed in the AER and loss of this gene widens the AER but does not disturb plantar–palmar patterning (Adamska et al., 2003), linking *Dkk1* with *Wnt5a* rather than *Wnt7a* activity. Similarly in the GT, loss of *Wnt5a* is also known to disrupt proximal–distal extension (Yamaguchi et al., 1999). *Wnt5a* expression has been reported to be expressed in the GT mesenchyme and appears to be regulated, along with *Msx2*, *Lef1*, and *Bmp4*, by signals from the distal urethral epithelium (Lin et al., 2008). Our data on *Wnt5a* agree with the literature in that expression was seen in the GT mesenchyme. Our clustering and expression analyses implied interaction between *Wnt5a* and other known Wnt pathway members, including *Frzb* (secreted frizzled related protein 3, Sfrp3), *Dkk1*, *Dkk2*, *Msx1*, *Tcfap2b*, and *Lef1*. An association between *Wnt5a* and *Frzb* in digit formation has already been described (Chimal-Monroy et al., 2002), supporting the validity of this cluster. Alignment of the expression patterns of these genes showed a distinct band of *Dkk1* expression delineating the boundary of the *Wnt5a* expression in the emerging glans region, presumably delimiting the boundary of *Wnt5a*-driven canonical Wnt signaling.

Differentiation between the plantar and palmar (dorsal and ventral) surface of the limb requires dorsal *Wnt7a* signaling accompanied by repression of that signal on the ventral surface by the transcription factor, engailed-1 (*En-1*; Geetha-Loganathan et al., 2008). Dorsal Lmx1b expression is also thought to be regulated by Wnt7a (Chen and Johnson, 2002; Geetha-Loganathan et al., 2008). Rare occasions have been reported where there has been a duplication of the palmar surface due to mutation in *Wnt7a* (Al-Qattan et al., 2009). The role of Wnt signaling in the developing ectoderm of the GT has not previously been investigated. Unlike the limb, *Wnt7a* expression was not restricted to the dorsal surface of the GT although in this region it did show a specific pattern of expression. Alignment of ISH and gene cluster analysis identified other genes expressed in the GT surface epithelium (*Sostdc1*, *Gjb2*, *Dsc3*, and *Krt5)*, most of which have known roles in epidermal differentiation in other tissues. *Gjb2* encodes a gap junction protein also called connexin 26. Mutations in connexin 26 result in deafness as a result of cornification of the epithelium within the cochlea of the ear (Richard, 2000; Houang et al., 2002). Connexin 26 and connexin 31 (*Gjb3*) are crucial for normal epidermal development, and as well as deafness, connexin 26 mutations can result in palmo-plantar keratoderma (Richard, 2000; de Zwart-Storm et al., 2008). *Dsc3* is a cadherin-like protein present in desmosomes and previously reported to be expressed in the epidermis of the foreskin (King et al., 1995). *Dsc3* is upregulated along with β-catenin in squamous cell carcinoma (Wang et al., 2007) and disruptions of squamous and stratified epithelium. This includes palmo-plantar keratoderma and immunobullous disease in a patient with circulating antibodies against *Dsc3* (Bolling et al., 2007). This patient presented hyperkeratotic ridges on their palms as well as intra-epidermal pustules. Based on these prior associations, we can predict that this cluster of genes is involved in differentiation of the epidermis of the GT but not necessarily the epithelium of the UP.

Genes within the predicted Wnt7a-associated network are known to be modulated by retinoic acid (RA) and diethylstilbestrol (DES). Sexual dimorphism of the external genitalia is dependent on steroid hormones and there have been many reports linking imbalance between estrogen and androgen signaling to hypospadias, including the use of DES during pregnancy (Brouwers et al., 2007). This is thought to affect development during the androgen-sensitive sexually dimorphic stage of GT development (>E16) rather than during early development. An association between these epidermal GT genes and DES implies either a previously unreported early estrogen-sensitive period or involvement in both the androgen-independent and subsequent androgen-sensitive phase of GT development. DES

exposure during development also results in metaplasia of the normally simple columnar epithelium of the uterus, thereby preventing embryo implantation (Huang et al., 2005). Here *Msx2* is required for normal *Wnt7a* expression and DES can repress the expression of both *Msx2* and *Wnt7a* in turn (Huang et al., 2005). This effect is mediated via the estrogen receptor, since ER-KO mice treated with DES do not show a reduction in *Wnt7a* (Couse and Korach, 2004). Hence, Wnt7a and other DES-responsive genes in this network may also be involved in female reproductive tract development. Sexual dimorphism of the external genitalia is also thought to involve RA signaling due to the dynamic expression of RARs, RXRs, RALDH2, and CYP26 (Ogino et al., 2001). Administration of RA to mouse embryos as young as E9 does not affect genital tubercle extension but does disrupt the formation of the urethral plate. Our reexamination of these data revealed undescribed defects in the development of the preputial swellings and the shape of the distal glans (Ogino et al., 2001). Studies on the effect of an absence of RA on limb development in the quail embryo showed that while all axes were disrupted, this particularly affected limb dorsal–ventral patterning genes, including *Wnt7a* and *En-1* (Stratford et al., 1999). While this does not eliminate a role for *Wnt7a* in other axes of GT development, it is suggestive of limb/GT congruence and strengthens the association between the genes in this cluster.

Overall, our observations suggest that *Wnt7a* may play a role in epidermal differentiation of the GT in collaboration with genes known to play roles in plantar–palmar epidermal dimorphism. The expression of Wnt7a-synexpressed genes in the epithelium of the preputial swelling may implicate this network in the differentiation of the foreskin and labia rather than in extension of the glans. This division of expression may serve to demarcate the development of the smooth skin of the penis and clitoris and the epidermis that will give rise to the foreskin, labia minora, and scrotum (Fig. 6A and B). The link to androgen regulation may also suggest that at least some forms of hypospadias or other congenital glans malformations may involve disruptions to epidermal development. Indeed, a review of 137 non-diphallic non-hypospadiac glans defects noted dermatological lesions in 15% of cases (Papali et al., 2008).

In this study, gene ontology, pathway, and network analysis of the microarray data have reinforced the concept of molecular congruence in appendage development. However, while initially arising as paired genital swellings, the glans in both sexes (penis and clitoris) becomes a single midline structure, unlike the limbs. Significant morphological differences exist between the dorsal and ventral surfaces of the developing limb, both externally with respect to skin, hair, and nail formation, and internally with respect to extensor and flexor muscle positioning. The same is true for the anterior–posterior axis of the limbs. This is not as prominent in the external genitalia. While duplication of the *Shh*-expressing ZPA on the posterior surface of the limb (duplication of the A–P axis) gives rise to a duplication of digits, a dorsal duplication of the *Shh*-expressing urethral plate never occurs. Duplication of the urethral plate can occur if there is an underlying duplication of the urethral endoderm, but this duplication occurs ventrally and gives rise to a total GT duplication, referred to as diphallia in males (Kaufman et al., 1990; Gyftopoulos et al., 2002; Mughal et al., 2003). This is usually accompanied by urethral or bladder duplication and imperforate anus. Such phallic duplications almost always occur in the lateral plane such that the two appendages are positioned side by side. Rare cases of duplication apparently in the dorsal–ventral axis usually involve incomplete or glans-only duplication with no accompanying urethral or bladder duplication (Melekos et al., 1986; Gavali et al., 2002). If the limb A–P axis is equivalent to GT D–V axis, lateral diphallia would be equivalent to a duplication of the hand in the D–V axis, which has never been reported. We therefore conclude that while early congruences in patterning exist between different appendages, particularly in relation to extension, there remain significant and anatomically obvious differences between these structures and hence the molecular regulation of these processes.

## Acknowledgments

We thank Emmanuelle Lesieur for assistance in material collection and Jane Brennan, Jane Armstrong, Chris Armit, Jamie Davies, Derek Houghton, Sue Lloyd-MacGilp, Mehran Sharghi, Xinguin Pi, Yogmatee Roochun, Ying Cheng, Simon Harding, Jamie Davies, and Duncan Davidson for GUDMAP editorial and database support. We also thank Carol Wicking for scientific opinion on limb and facial development. ML is a Principal Research Fellow of the National Health and Medical Research Council. This work was supported by the National Institutes of Health via awards DK070136 (MHL) and DK070219 (JLL).

## Appendix A. Supplementary data

Supplementary data associated with this article can be found, in the online version, at doi:10.1016/j.ydbio.2010.05.495.

## References

Aboushwareb, T., Zhou, G., Deng, F.M., Turner, C., Andersson, K.E., Tar, M., Zhao, W., Melman, A., D'Agostino Jr., R., Sun, T.T., Christ, G.J., 2009. Alterations in bladder function associated with urothelial defects in uroplakin II and IIIa knockout mice. Neurourol Urodyn, Epub ahead of print.

Adamska, M., MacDonald, B.T., Meisler, M.H., 2003. Doubleridge, a mouse mutant with defective compaction of the apical ectodermal ridge and normal dorsal–ventral patterning of the limb. Dev. Biol. 255, 350–362.

Ahn, K., Mishina, Y., Hanks, M.C., Behringer, R.R., Crenshaw, E.B.I.I.I., 2001. BMPR-1A signaling is required for the formation of the apical ectodermal ridge and dorsal–ventral patterning of the limb. Development 128, 4449–4451.

Al-Qattan, M.M., Al-Balwi, M., Eyaid, W., Al-Abdulkarim, I., Al-Turki, S., 2009. Congenital duplication of the palm syndrome: gene analysis and the molecular basis of its clinical features. J. Hand Surg. 34E, 247–251.

Beleza-Meireles, A., Lundberg, F., Lagerstedt, K., Zhou, X., Omrani, D., Frisen, L., Norddenskjold, A., 2007. FGFR2, FGF8, FGF10 and BMP7 as candidate genes for hypospadias. Eur. J. Hum. Genet. 15, 405–410.

Bogart, M.M., Arnold, H.E., Greer, K.E., 2006. Prune-belly syndrome in two children and review of the literature. Pediatr. Dermatol. 23, 342–345.

Bolling, M.C., Mekkes, J.R., Goldschmidt, W.F., van Noesel, C.J., Jonkman, M.F., Pas, H.H., 2007. Acquired palmoplantar keratoderma and immunobullous disease associated with antibodies to desmocollin 3. Br. J. Dermatol. 157, 168–173.

Brouwers, M.M., Feitz, W.F., Roelofs, L.A., Kiemeney, L.A., de Gier, R.P., Roeleveld, N., 2007. Risk factor for hypospadias. Eur. J. Pediatr. 166, 671–678.

Brunskill, E.W., Aronow, B.J., Georgas, K., Valerius, M.T., Aronow, J.E., Kaimal, V., Jegga, A.G., Grimmond, S., McMahon, A.P., Patterson, L., Little, M.H., Potter, S.S., 2008. Atlas of gene expression in developing kidney at microanatomic resolution. Dev. Cell 15, 781–791.

Chen, H., Johnson, R.L., 2002. Interactions between dorsal–ventral patterning genes lmx1b, engrailed-1 and wnt-7a in the vertebrate limb. Int. J. Dev. Biol. 46, 937–941.

Chen, J., Bardes, E.E., Aronow, B.J., Jegga, A.G., 2009. ToppGene Suite for gene list enrichment analysis and candidate gene prioritization. Nucleic Acids Res. 37, W305–W311 Web Server issue.

Chimal-Monroy, J., Montero, J.A., Gañan, Y., Macias, D., Garcia-Porrero, J.A., Hurle, J.M., 2002. Comparative analysis of the expression and regulation of Wnt5a, Fz4, and Frzb1 during digit formation and in micromass cultures. Dev. Dyn. 224 (3), 314–320.

Cobb, J., Duboule, D., 2005. Comparative analysis of genes downstream of the Hoxd cluster in developing digits and external genitalia. Development 132, 3055–3067.

Cobb, J., Dierich, A., Huss-Garcia, Y., Duboule, D., 2006. A mouse model for human short-stature syndromes identifies Shox2 as an upstream regulator of Runx2 during long-bone development. Proc. Natl Acad. Sci. U S A. 103, 4511–4515.

Couse, J.F., Korach, K.S., 2004. Estrogen receptor-alpha mediates the detrimental effects of neonatal diethylstilbestrol (DES) exposure in the murine reproductive tract. Toxicology 205, 55–63.

Cox, M.J., Coplen, D.E., Austin, P.F., 2008. The incidence of disorders of sexual differentiation and chromosomal abnormalities of cryptorchidism and hypospadias stratified by meatal location. J. Urol. 180, 2649–2652.

De Zwart-Storm, E.A., van Geel, M., van Neer, P.A., Steijlen, P.M., Martin, P.E., van Steensel, M.A., 2008. A novel missense mutations in the second extracellular domain of GFB2, p.Ser183Phe, causes a syndrome of focal palmoplantar keratoderma with deafness. Am. J. Pathol. 173 (4), 1113–1119.

Fowler, C.J., Griffiths, D., de Groat, W.C., 2008. The neural control of micturition. Nat. Rev. 9, 453–466.

Gavali, S., Deshpande, A.V., Sanghani, H.H., Hirugade, S.T., Talpallikar, M.C., Borwankar, S.S., 2002. Glanular diphallus with urethral stricture. Pediatr. Surg. Int. 18, 70–71.

Geetha-Loganathan, P., Nimmagadda, S., Scaal, M., 2008. Wnt signaling in limb organogenesis. Organogenesis 4 (2), 109–115.

Goodman, F.R., Bacchelli, C., Brady, A.F., Brueton, L.A., Fryns, J.P., Mortlock, D.P., Innis, J.W., Holmes, L.B., Donnenfeld, A.E., Feingold, M., Beemer, F.A., Hennekam, R.C., Scambler, P.J., 2000. Novel HOXA13 mutations and the phenotypic syndromeof hand–foot–genital syndrome. Am. J. Hum. Genet. 67, 197–202.
Gyftopoulos, K., Wolffenbuttel, K.P., Nijman, R.J., 2002. Clinical and embryologic aspects of penile duplication and associated anomalies. Urology 60 (4), 675–679.
Haraguchi, R., Suzuki, K., Murakami, R., Sakai, M., Kamikawa, M., Kengaku, M., Sekine, K., Kawano, H., Kato, S., Ueno, N., Yamada, G., 2000. Molecular analysis of external genitalia formation: the role of fibroblast growth factor (Fgf) genes during genital tubercle formation. Development 127 (11), 2471–2479.
Haraguchi, R., Mo, R., Hui, C., Motoyama, J., Makino, S., Shiroishi, T., Gaffield, W., Yamada, G., 2001. Unique functions of Sonic hedgehog signaling during external genitalia development. Development 128 (21), 4241–4250.
Hill, T.P., Taketo, M.M., Birchmeier, W., Hartmann, C., 2006. Multiple roles of mesenchymal beta-catenin during limb patterning. Development 133, 1219–1229.
Houang, M., Gourmelen, M., Moatti, L., Le, B.Y., Garabédian, E.N., Denoyelle, F., 2002. Hypogonadotrophic hypogonadism associated with prelingual deafness due to a connexin 26 gene mutation. J. Pediatr. Endocrinol. Metab. 15 (2), 219–223.
Huang, W.W., Yin, Y., Bi, Q., Chiang, T.C., Vuoristo, J., McLachlan, J.A., Ma, L., 2005. Developmental diethylstilbestrol exposure alters genetic pathways of uterine cytodifferentiation. Mol. Endocrinol. 19, 669–682.
Kalfa, N., Liu, B., Ophir, K., Audran, F., Wang, M.-H., Mei, C., Sulton, C., Baskin, L.S., 2008. Mutations of CXorf6 are associated with a range of severities of hypospadias. Eur. J. Endocrinol. 159, 452–458.
Kaufman, M., 1994. The atlas of mouse development. Academic Press, London.
Kaufman, A., Guia, R., Davila, H., Kaufman, A., 1990. Diphallus with third urethra. Urology 35 (3), 257–260.
Kerecuk, L., Schreuder, M.F., Woolf, A.S., 2008. Renal tract malformations: perspectives for nephrologists. Nat. Clin Pract. 4, 312–325.
King, I.A., Sullivan, K.H., Bennett Jr., R., Buxton, R.S., 1995. The desmocollins of human foreskin epidermis: identification and chromosomal assignment of a third gene and expression patterns of the three isoforms. J. Investig. Dermatol. 105 (3), 314–321.
Kurzrock, E.A., Baskin, L.S., Cunha, G.R., 1999. Ontogeny of the male urethra: theory of endodermal differentiation. Differentiation 64, 115–122.
Li, J., Willingham, E., Baskin, L.S., 2006. Gene expression profiles in mouse urethral development. BJU Int. 98, 880–885.
Lin, C., Yin, Y., Long, F., Ma, L., 2008. Tissue-specific requirements of β-catenin in external genitalia development. Development 135, 2815–2825.
Lin, C., Yin, Y., Veith, G.M., Fisher, A.V., Long, F., Ma, L., 2009. Temporal and spatial dissection of Shh signaling in genital tubercle development. Development 136, 3959–3967.
Little, M.H., Brennan, J., Georgas, K., Davies, J., Davidson, D., et al., 2007. A high-resolution anatomical ontology of the developing murine genitourinary tract. Gene Expr. Patterns 7 (6), 680–699.
Mariani, F.V., Ahn, C.P., Martin, G.R., 2008. Genetic evidence that FGFs have an instructive role in limb proximal–distal patterning. Nature 453 (7193), 401–405.
McMahon, A.P., Aronow, B.J., Davidson, D.R., Davies, J.A., Gaido, K.W., Grimmond, S., Lessard, J.L., Little, M.H., Potter, S.S., Wilder, E.L., Zhang, P., 2008. GUDMAP: the genitourinary developmental molecular anatomy project. J. Am. Soc. Nephrol. 19 (4), 667–671.
Melekos, M.D., Barbalias, G.A., Asbach, H.W., 1986. Penile duplication. Urology 27 (3), 258–259.
Miyagawa, S., Buchanan, D.L., Sato, T., Ohta, Y., Nishina, Y., Iguchi, T., 2002. Characterization of diethylstilbestrol-induced hypospadias in female mice. Anat. Rec. 266, 43–50.
Miyagawa, S., Moon, A., Haraguchi, R., Inoue, C., Harada, M., Nakahara, C., Suzuki, K., Matsumaru, D., Kaneko, T., Matsuo, I., Yang, L., Taketo, M.M., Iguchi, T., Evans, S.M., Yamada, G., 2009. Dosage-dependent hedgehog signals integrated with Wnt/b-catenin signaling regulate external genitalia formation as an appendicular program. Development 136, 3969–3978.
Morgan, E.A., Nguyen, S.B., Scott, V., Stadler, H.S., 2003. Loss of Bmp7 and Fgf8 signaling in Hoxd13-mutant mice causes hypospadias. Development 130, 3095–3109.
Mughal, S.A., Soomro, S., Shaikh, J.M., 2003. Double phallus. J. Coll. Physicians Surg. Pak. 13 (9), 534–535.
Nakata, M., Takada, Y., Hishiki, T., Saito, T., Terui, K., Sato, Y., Koseki, H., Yoshida, H., 2009. Induction of Wnt5a-expressing mesenchymal cells adjacent to the cloacal plate is an essential process for its proximodistal elongation and subsequent anorectal development. Pediatr. Res. 66 (2), 149–154.
Ogino, Y., Suzuki, K., Haraguchi, R., Satoh, Y., Dolle, P., Yamada, G., 2001. External genitalia formation: role of fibroblast growth factor, retinoic acid and distal urethral epithelium. Ann. NY Acad. Sci. 948, 13–31.
Papali, A.C., Alpert, S.A., Edmondson, J.D., Maizels, M., Yerkes, E., Hagerty, J., Chaviano, A., Kaplan, W.E., 2008. A review of pediatric glans malformations: a handy clinical reference. J. Urol. 180, 1737–1742.
Pennington, E.C., Hutson, J.M., 2002. The urethral plate—does it grow into the genital tubercle or within it? BJU Int. 89, 733–739.
Perriton, C.L., Powles, N., Chiang, C., Machonochie, M.K., Cohn, M.J., 2002. Sonic hedgehog signaling from the urethral epithelium controls external genital development. Dev. Biol. 247 (1), 26–46.
Richard, G., 2000. Connexins: a connection with the skin. Exp. Dermatol. 9 (2), 77–96.
Saha, S.R., Roy, A.K., Saha, S., 2005. Incidence of associated congenital anomalies in anorectal malformations. J. Indian Med. Assoc. 103, 690–691.
Salerno, A., Kohlhase, J., Kaplan, B.S., 2000. Townes–Brocks syndrome and renal dysplasia: a novel mutation in the SALL1 gene. Pediatr. Nephrol. 14, 25–28.
Schneider, R.A., Hu, D., Helms, J.A., 1999. From head to toe: conservation of molecular signals regulating limb and craniofacial morphogenesis. Cell Tissue Res. 296 (1), 103–109.
Siefert, A.W., Harfe, B.D., Cohn, M.J., 2008. Cell lineage analysis demonstrated an endodermal origin of the distal urethra and perineum. Dev. Biol. 318, 143–152.
Siefert, A.W., Yamaguchi, T., Cohn, M.J., 2009. Functional and phylogenetic analysis shows that Fgf8 is a marker of genital induction in mammals but is not required for external genital development. Development 136, 2643–2651.
Stratford, T., Logan, C., Zile, M., Maden, M., 1999. Abnormal anteroposterior and dorsoventral patterning of the limb bud in the absence of retinoids. Mech. Dev. 81, 115–125.
Suzuki, K., Bachiller, D., Chen, Y.P., Kamikawa, M., Ogi, H., Haraguchi, R., Ogino, Y., Minami, Y., Mishina, Y., Ahn, K., Crenshaw 3rd, E.B., Yamada, G., 2003. Regulation of outgrowth and apoptosis for the terminal appendage: external genitalia development by concerted actions of BMP signaling. Development 130 (25), 6209–6220.
Suzuki, K., Haraguchi, R., Ogata, T., Barbieri, O., Alegria, O., Vieux-Rochas, M., Nakagata, N., Ito, M., Mills, A.A., Kurita, T., Levi, G., Yamada, G., 2008. Abnormal urethra formation in mouse models of split-hand/split-foot malformation type 1 and type 4. Eur. J. Hum. Genet. 16, 36–44.
Szucsik, J.C., Lewis, A.G., Marmer, D.J., Lessard, J.L., 2004. Urogenital tract expression of enhanced green fluorescent protein in transgenic mice driven by a smooth muscle gamma-actin promoter. J. Urol. 171 (2 Pt 1), 944–949.
Trumpp, A., Depew, M.J., Rubenstein, J.L.R., Bishap, J.M., Martin, G.R., 1999. Cre-mediated gene inactivation demonstrates that FGF8 is required for cell survival and patterning of the first branchial arch. Genes Dev. 13, 3136–3148.
Wang, M.-H., Baskin, L.S., 2008. Endocrine disruptors, genital development and hypospadias. J. Androl. 29, 499–505.
Wang, L., Liu, T., Wang, Y., Cao, L., Nishioka, M., Aguirre, R.L., Ishikawa, A., Geng, L., Okada, N., 2007. Altered expression of desmocollin 3, desmoglein 3 and beta-catenin in oral squamous cell carcinoma: correlation with lymph node metastasis and cell proliferation. Virchows Arch. 451 (5), 959–966.
Weber, S., Mir, S., Schlingmann, K.P., Nurnberg, G., Becker, C., Kara, P.E., Ozkayin, N., Konrad, M., Nurnberg, P., Schaefer, F., 2005. Gene locus ambiguity in posterior urethral valves/prune belly syndrome. Pediatr. Nephrol. 20, 1036–1042.
Weber, S., Moriniere, V., Knüppel, T., Charbit, M., Dusek, J., Ghiggeri, G.M., Jankauskiené, A., Mir, S., Montini, G., Peco-Antic, A., Wühl, E., Zurowska, A.M., Mehls, O., Antignac, C., Schaefer, F., Salomon, R., 2006. Prevalence of mutations in renal developmental genes in children with renal hypodysplasia: results of the ESCAPE study. J. Am. Soc. Nephrol. 17, 2864–2870.
Witte, F., Dokas, J., Neuendorf, F., Mundlos, S., Stricker, S., 2009. Comprehensive expression analysis of all Wnt genes and their major secreted antagonists during mouse limb development and cartilage differentiation. Gene Expr. Patterns 2, 215–223.
Yamada, G., Suzuki, K., Haraguchi, R., Miyagawa, S., Satoh, Y., Kamimura, M., Nakagata, N., Kataoka, H., Kuroiwa, A., Chen, Y., 2006. Molecular genetic cascades for external genitalia formation: an emerging organogenesis program. Dev. Dyn. 235, 1738–1752.
Yamaguchi, T.P., Bradley, A., McMahon, A.P., Jones, S.A., 1999. Wnt5a pathway underlies outgrowth of multiple structures in the vertebrate embryo. Development 126, 1211–1223.